Graduate Theses and Dissertations   Graduate School

2011

Polydimethylsiloxane Mechanical Properties Measured by Macroscopic Compression and Nanoindentation Techniques

Zhixin Wang
University of South Florida, zwang3@mail.usf.edu

Polydimethylsiloxane Mechanical Properties Measured by Macroscopic Compression and

Nanoindentation Techniques

by

Zhixin Wang

A thesis submitted in partial fulfillment
of the requirements for the degree of
Master of Science in Mechanical Engineering
Department of Mechanical Engineering
College of Engineering
University of South Florida

Co-Major Professor: Alex. A. Volinsky, Ph.D.
Co-Major Professor: Nathan Gallant, Ph.D.
Delcie Durham, Ph.D.

Date of Approval:
March 23, 2011

Keywords: soft material, elastic modulus, adhesion force, flat punch, DMA

Dedication

I would like to dedicate this manuscript to my relatives, especially my parents.

Thank you for all your support and encouragement throughout the years.

Acknowledgements

I would like to thank my advisor Dr. Volinsky. Without his guidance, this thesis could not be published. I also want to thank my advisor Dr. Gallant for providing valuable suggestions in my research work and thesis writing.

Table of Contents

List of Tables

List of Figures

Abstract

In this thesis, the relationship between the elastic modulus of PDMS and the base/agent ratio (the amount of crosslinking) is studied. Reliable macroscopic compression test instrument was developed. Preload method was applied for the nanoindentation flat punch test to develop full contact.

In chapter 2, an easy instrument setup for macroscopic compression test is described. A series of PDMS samples with different base/agent ratios were tested using the macroscopic compression method. The relationship between PDMS elastic modulus and its base/agent ratio was established.

In chapter 3, PDMS nanoindentation DMA tests provide stable data with different test control models. The storage modulus collected using nanoindenting DMA tests is comparable with elastic modulus collected in PDMS compression test in chapter 2. Nanoindentation experiments with flat punch were also done to test the elastic modulus of PDMS network 5:1. The adhesion force tests with different nanoindentation tips, which are Berkovich tip, conical tip and cube corner tip, show that PDMS's adhesion force is related to the sample's base/agent ratio, the nanoindentating depth and the tip's geometrical shape.

Chapter 1. Introduction to PDMS Mechanical Properties

1.1 Introduction to Polymers Mechanical Properties

Polymers are not as stiff as metals and ceramics, but not as soft as liquids. Polymers' mechanical properties are different from others types of materials.

1.1.1 Elastic Modulus of Polymers

Modulus is one of the most important materials' properties. For an ideal elastic solid, Hooke's law expresses the Young's modulus, E, as

$$E=\sigma/\varepsilon \tag{1},$$

here, σ is the stress and ε is the strain. Stress and strain can be either tensile or compressive. From Equation (1), one can get the material's stiffness - its Young's modulus. Stress σ is force per unit area and strain ε is length change per unit length, that is $\varepsilon=(L-L_0)/L_0$, it is easy to understand that for the same strain, the larger the stress is, the stiffer the material is (the larger the Young's modulus is).

For an ideal viscous liquid, Newton's law expresses the shear viscosity, η, defined as:

$$\eta=\tau /(d\gamma/dt) \tag{2},$$

where, τ represents the shear stress and γ represents the shear strain, and t is the time. For simple liquids such as water or toluene, Equation (2) reasonably describes their viscosity, especially at low shear rates. For larger values of η, flow is slower at constant shear stress [1].

1

Equation (1) describes the mechanical properties of ideal elastic solids, while Equation (2) is suitable for ideal viscous liquids. Figures 1 and 2 show this in more detail and represent the two limiting cases.
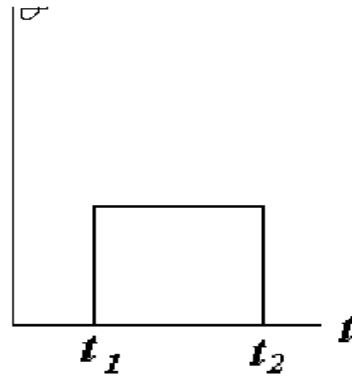
Figure 1.a. Stress-time behavior of an ideal elastic solid.
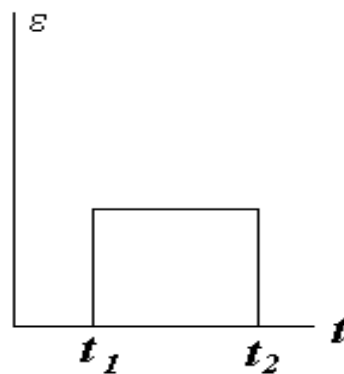
Figure 1.b. Strain-time behavior of an ideal elastic solid.

2
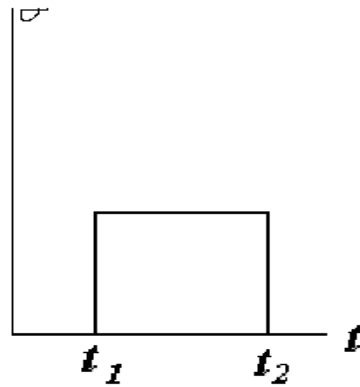
Figure 2.a. Stress-time behavior of an ideal viscous solid.
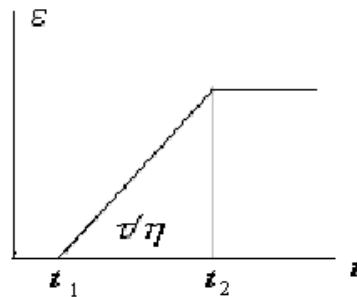
Figure 2.b. Strain-time behavior of an ideal viscous solid.

Equations (1) and (2) neither can accurately describe the mechanical behavior of polymers. For polymers, the suitable complex Young's modulus is defined as:

$$E^* = E' + iE''$$ (3),

where E' is the storage modulus and E'' is the loss modulus [1]. Note that $E = |E^*|$. The quantity i represents the square root of minus one. The storage modulus is a measure of the energy stored elastically during deformation, and the loss modulus is a measure of the energy converted to heat. Similar definitions hold for G* (complex shear modulus) and other mechanical quantities.

3

Deformed molecules store a portion of the energy elastically and dissipate a portion in the form of heat. The quantity E', storage modulus, is a measure of the energy stored elastically, whereas E'', loss modulus, is a measure of the energy lost as heat.

1.1.2 Viscoelasticity

As discussed above, complex modulus can describe the mechanical properties of polymers. Also, the complex modulus describes viscoelasticity of polymers, which is a basic and specific property of polymers. There are two basic models of viscoelasticity, namely Maxwell and Kelvin-Voigt models. [2]

Viscoelasticity results in a lot of interesting phenomena in polymers. For example, creep and stress relaxation represent the static viscoelasticity, while lag and internal friction can describe the dynamic viscoelasticity [3]. Viscoelasticity can be studied with dynamic mechanical analysis (DMA) utilizing Hysitron TriboIndentor.

1.2 Introduction to PDMS

The material for research in this thesis is Polydimethylsiloxane (PDMS), which is a silicone-based polymer. PDMS is the most widely used silicon-based organic polymer, and is particularly known for its unusual rheological (or flow) properties. Its applications range from contact lenses and medical devices to elastomers. It is also found in shampoos (dimethicone makes hair shiny and slippery), caulking, lubricating oils and heat resistant tiles. PDMS is optically clear, and is generally considered to be inert, non-toxic and non-flammable. It is occasionally called dimethicone and is one of several types of silicone oil (polymerized siloxane) [4-6].

4

Silane precursors with more acid-forming groups and fewer methyl groups, such as methyltrichlorosilane, can be used to introduce branches or cross-links in the polymer chains. Ideally, each molecule of such a compound becomes a branch point. This can be used to produce hard silicone resins.

PDMS network can be used as substrate to grow cells. Varying the crosslink density in the polymer network allows one to tune the mechanical properties in a range similar to living tissues. The effect of PDMS network stiffness on the growth and behavior of cells is studied. The main focus of this thesis is to characterize the local surface mechanical properties of a series of PDMS network samples, which are cured to different crosslink densities. Both macroscopic compression and nanoindentation tests were used in this project.

1.2.1 Microstructure of PDMS

The chemical formula for PDMS is $(H_3C)_3SiO[Si(CH_3)_2O]nSi(CH_3)_3$, where n is the number of repeating monomer $[SiO(CH_3)_2]$ units. Its brief formula is shown in Figure 3. Industrial synthesis starts from dimethylchlorosilane and water following the reaction:

$$n\ Si(CH_3)_2Cl_2 + n\ H_2O \rightarrow [Si(CH_3)_2O]_n + 2n\ HCl \qquad (4).$$
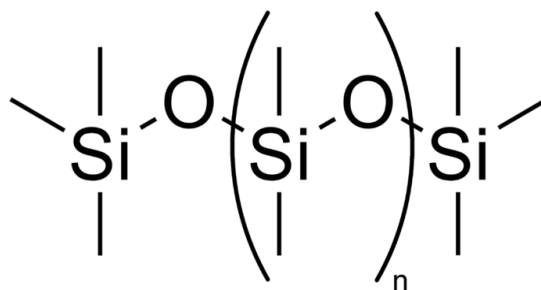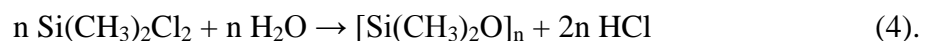
Figure 3. PDMS chemical formula [6].

Network of PDMS polymer is assembled by crosslinking these polymer chains. The long PDMS polymer chains usually have vinyl groups at each end. The short crosslinker is polymethylhydro- siloxane, which links the PDMS chains. This reaction can be catalyzed by platinum.

1.2.2 Samples for Research

PDMS network samples for this research were synthesized with the same composition, which are Sylgard 184 silicone elastomer base and Sylgard 184 silicone elastomer curing agent [7]. These samples have different base/agent ratios, which mean different degrees of cross-linking. The lower the degree of PDMS network's cross-linking, the softer PDMS network is. Conversely, the higher the degree of cross-linking, the stiffer the sample will be. Samples' stiffness was varied by changing the ratio of crosslinker to base polymer in this thesis.

The most widely used type of PDMS network in research is PDMS 10:1, which means ten mass of Sylgard 184 silicone elastomer base with 1 mass of Sylgard 184 silicone elastomer curing agent. For PDMS network, different base/agent ratio means different amount of cross-linking. For this research, a series of PDMS network samples with different base/agent ratios are used to explore the relationship between modulus changing and the different amount of PDMS network's cross-linking, which are PDMS network 5:1, PDMS network 7:1, PDMS network 10:1, PDMS network 16.7:1, PDMS network 25:1 and PDMS network 33:1 [7-8].

Different sizes of samples are made for different uses. One part of this research is macroscopic compression testing, the samples for which are cylinders, with length/diameter ratio less than 2. The other part is nanoindentation based testing, for which samples are $1 \times 1 cm^2$ squares with the same thickness as samples used in

6

macroscopic compression testing. Hysitron Triboindenter has DMA system, which is designed for soft materials' complex modulus testing [9]. These two experimental methods will be described in the following chapters in more details.

The samples used for this research have different amounts of crosslinking. Varying the crosslink density in the polymer network allows one to tune the mechanical properties in a range similar to living tissues. During the tests, one can get the elastic modulus and complex modulus of these samples, compare the data within different test methods and obtain the relationship between PDMS network mechanical properties and its amount of crosslinking.

1.3 The Objectives and Challenges for This Research

Therefore, the goals of this thesis are: measuring mechanical properties of PDMS network of varied crosslinking density and adapting nanoindenter to analyse soft materials' mechanical properties.

The testing of PDMS network mechanical properties is quite novel, and there are not many literature references. The challenges are mostly about two aspects. First, traditional mechanical properties testing machines do not work for these soft PDMS samples. Typical instruments cannot provide low force control system and cannot easily measure the significant displacement during polymer testing [10-12]. To conventional DMA testing, the instrument is complicated to control and the testing process depends too much on the testing temperature. Second, PDMS network is soft, and its elastic modulus is less than 5 MPa. It is not easy to develop full contact in the beginning of the experiment and it is challenging to make standard specimen shape for mechanical properties testing [13, 14].

7

Chapter 2. Macroscopic Compression Testing

2.1 Introduction to Tension and Compression Tests

For almost all metals, one can get their elastic modulus and yield stress with a simple tensile test. Mild steel tensile test result is shown in Figure 4.
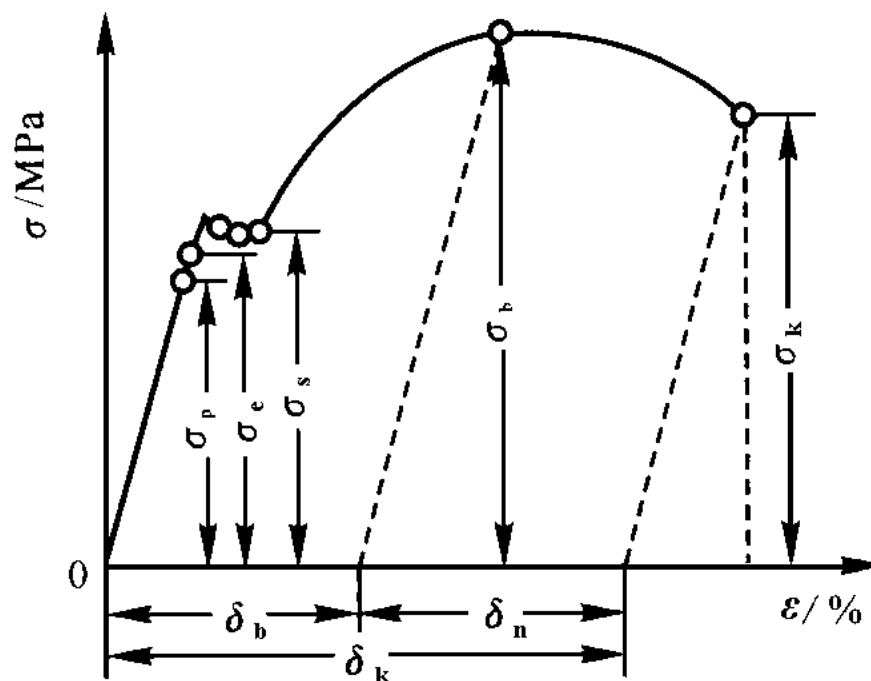
Figure 4. Mild steel tensile test stress-strain curve.

In Figure 4, stress σ is the average normal stress, i.e. normal force per unit area of the sample cross-section. Stress SI units are Pascals (Pa). δ is the sample length change during the tensile test. Strain ε is the length change per unit length. σ_p is the proportional limit, which is the upper stress limit to the linear relationship. σ_e is the elastic stress, past which material is yielding, and the corresponding deformation is

8

called plastic deformation. The rise in the curve is called strain hardening, and σ_b is called the ultimate stress. At σ_b, the cross-sectional area begins to decrease in a localized region of the specimen, instead of over its entire length, called necking [15]. σ_k is called fracture stress, which happens when the specimen breaks.

The tensile test curve is different for different materials. For example, for more ductile materials, proportional limit is lower, while for brittle materials, there will be no necking.
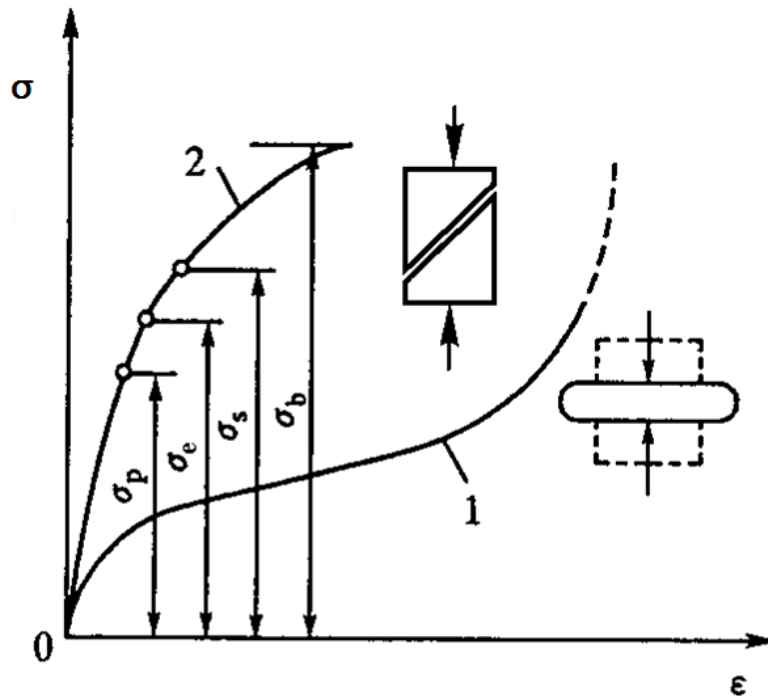
Figure 5. Compression test stress-strain curve.

Compression testing is the opposite of tensile testing, but can describe the same properties of materials. In Figure 5, the σ_p, σ_e, σ_s and σ_b have the same engineering meanings as in Figure 4.

9

In this thesis research, compression testing is applied for experiments because it is more suitable for soft PDMS network samples. The polymer samples' deformation process is much closer to that shown in Figure 5.

2.2 Samples and Instrumentation

2.2.1 Samples Preparation

Sylgard 184 silicone elastomer base and Sylgard 184 silicone elastomer curing agent were used to make PDMS. In Figure 6.a., a massive PDMS network sample is made using a flat Petri dish whose thickness is around 3 mm.

According to popular PDMS network curing procedure [16], PDMS network is cured as following:

1. Materials and equipment used: Sylgard 184 silicone elastomer base, Sylgard 184 silicone elastomer curing agent, petri dishes, wood spoons, plastic cups, vacuum desiccator, scale, hot plate, gloves.

2. Place the plastic cup onto the scale and tare.

3. Pour 27 g of the Sylard184 silicone elastomer base into the cup. Tare. Slowly pour 2.7 g of the Sylard 184 silicone elastomer curing agent into the same mix with the spoon (about 10 min, until mixture is milky due to air bubbles).

4. Put the PDMS mixture (in the cup) into the desiccator and turn the vacuum back on. De-gas the mixture under vacuum until no bubbles appear (20~30 min). Make sure the PDMS mixture does not foam out of the container. When large bubbles form at the surface, vent vacuum to pop bubbles.

5. Carefully pour PDMS over a Petri dish (try to minimize introduction of bubbles).

6. Place the Petri dish onto a hot plate (keep horizontally), set the hot plate at 65 °C, let PDMS network cure for 12 hours.

After PDMS network mold cures, the sample is stable and can be stored for months. The ratio between the initial length L_0 and the diameter D of the sample is a pertinent parameter. [17] In reference of ASM handbook -- Mechanical Testing and Evaluation, the length/diamater ratio for soft material compression sample should be less than 2. [18] So punches with 3 mm or 4 mm diameter were used to cut cylindrical PDMS network samples. In Figure 6.b., the different sizes of cylinder PDMS network samples are shown with clear details. With micrometer calipers, the length and diameter of cylinderical samples were measured accurately.

Figure 6.a. The massive PDMS network sample.

Figure 6.b. Cylindrical PDMS network samples for compression tests.

2.2.2 Instrument Design

Different kinds of compression testing machines can be used to measure materials' mechanical properties: SANS range of compression testing machines (Australia), Universal Compression Testing Machine (SYE-2000) (China), etc. For PDMS, it is not realistic to place samples in heavy load machines. Thus a more suitable instrument was designed for PDMS network compression testing based on the scale and displacement gauge [19, 20].
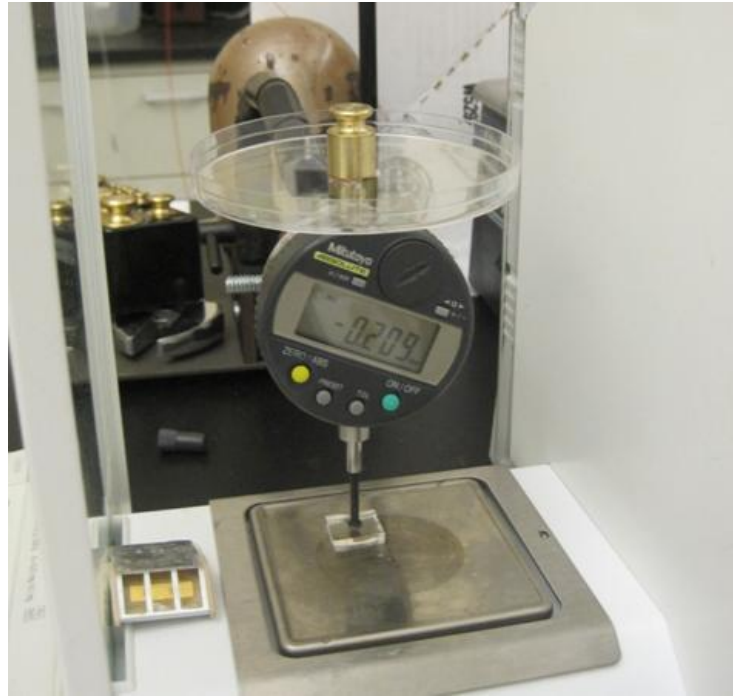
Figure 7. The instrument setup for macroscopic tests.

In Figure 7, the force is measured by the scale under the sample, while displacement is measured by the gauge above the sample. Weights are used to apply force to samples. The data shown in the scale is almost the same with the weight, which means the scale can be removed from this instrument set. (Shown in Figure 8) To reduce the error, the gauge shall be straight all the time during the experiment.

In experiments, calibration is made due to the spring in the gauge. After the spring was removed, the weight added on the gauge is exactly the force yielding on the sample. The instrument set was updated again shown in Figure 8.

13

Figure 8. Updated instrument setup.

Another calibration is made due to the movable metal connection, which holds the gauge in Figure 8. The movable joint connection caused 5 percent of the load deviation, so the instrument was simplified further, shown in Figure 9.

Figure 9. The final version of the instrument setup.

14

In Figure 9, the weight above the gauge applied the force to the sample in the compression testing. The sample is fully contacted with the metal stage, so the gauge can measure the displacement of the sample during compression.

Also, because the sample is soft, it is not easy to develop full contract between the gauge and the sample. To avoid this problem, the testing force of this experiment always started at 50 g [21].

2.2.3 Analysis Method

With the designed instrument setup, one can get the stress and strain of the sample:

$$\text{Stress } \sigma = m*9.8/(\pi*(D/2)^2) \qquad (5),$$

$$\text{Strain } \varepsilon = dL/L_0 \qquad (6),$$

where, m is the mass above the gauge, which applies the force to the sample. D is the diameter of the sample. dL is the change in the sample's length under compressive force. From Equation (1), it is easy to see the slope of stress-strain curve is the elastic modulus of the sample. More details are shown in figure 10.
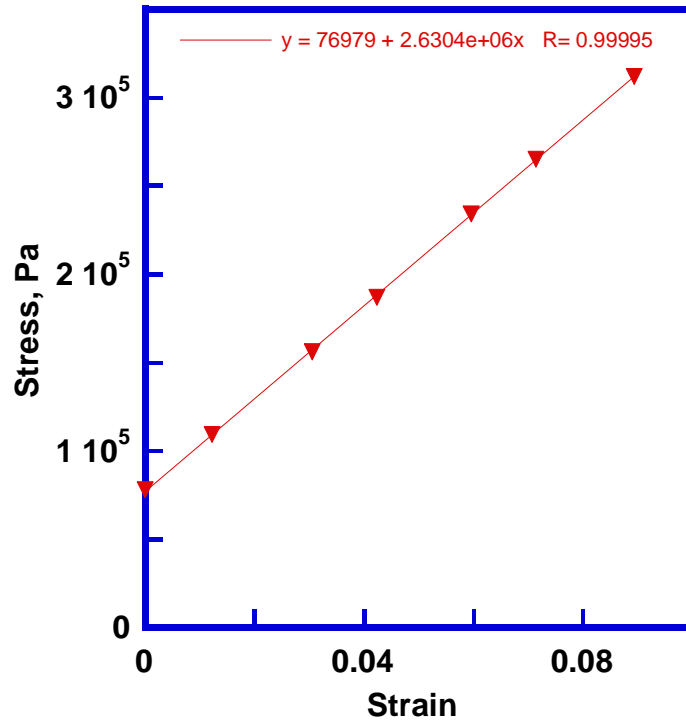
Figure 10. PDMS network 10:1 macroscopic compression test results.

Figure 10 is the data of compression test for standard PDMS network 10:1, after linearly fitting the data, the slope of the straight line is 2.63E+06 Pa, which means that elastic modulus of 10:1 PDMS network sample is 2.63 MPa.

16

2.3 Experiments and Data for Macroscopic Compression Testing

With the designed instrument setup and cylinderical PDMS network samples, compression tests were performed on a series of PDMS network samples.

2.3.1 PDMS Network Sample 5:1

PDMS network 5:1 is made of 17 g Sylgard 184 silicone elastomer base and 3.4 g Sylgard 184 silicone elastomer curing agent. After the sample cured completely, it was carefully cut and removed out of the Petri dish. Punches with 3 mm and 4 mm diameters were used to cut cylindrical sample. The most uniform cylinders were picked from all the samples. More details about the cylinder samples used in this macroscopic compression testing are shown in Table 1.

Table 1. Macroscopic compression test of PDMS network 5:1.

	Sample 1	Sample 2	Sample 3	Sample 4
Thickness, mm	2.808	2.834	2.853	2.825
Diameter, mm	3.849	3.82	2.848	2.828
Diameter/Thickness Ratio	1.371	1.348	0.998	1.001

Using the same testing method as described in section 2.2.3, the compression testing curve for PDMS network 5:1 sample 1 is shown in Figure 11.

17
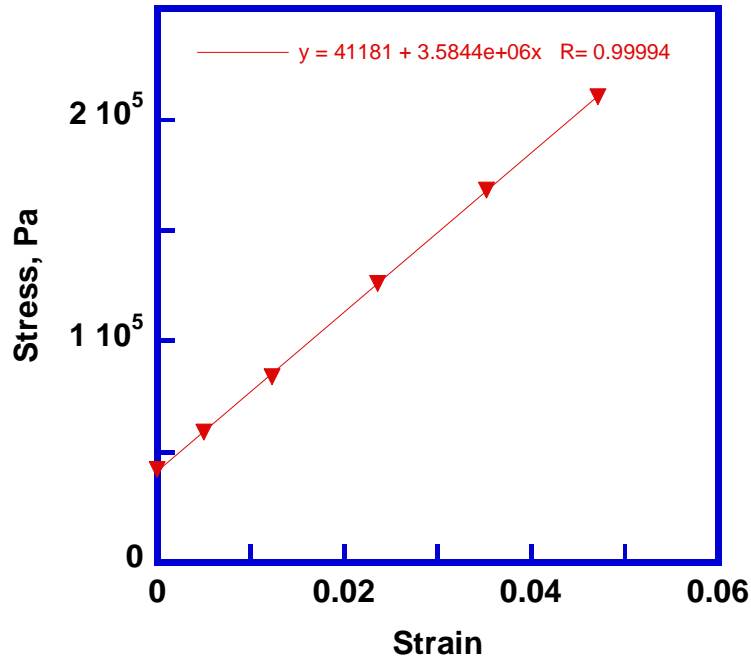
Figure 11. Compression test of PDMS network 5:1 sample 1.

In Figure 11, after linearly fitting the data, the slope of the straight line is 3.584E+6 Pa, which means the elastic modulus of PDMS network 5:1 sample 1 is 3.584 MPa.

In the same way, elastic modulus of sample 2, sample 3 and sample 4 were obtained: 3.728 MPa, 3.458 MPa and 3.582 MPa. Elastic modulus measurement results of PDMS network 5:1 are summarized in Table 2 and Figure 12.

Table 2. Elastic modulus of PDMS network 5:1.

	Sample 1	Sample 2	Sample 3	Sample 4
Elastic Modulus, MPa	3.584	3.728	3.458	3.582

Thus,

$$E_{average} = (E_1 + E_2 + E_3 + E_4)/4 = 3.588 \text{ Mpa} \tag{7}$$

18

The standard deviation, δ, is:

$$\delta = \sqrt{\frac{(E_1 - E_{ave})^2 + (E_2 - E_{ave})^2 + (E_3 - E_{ave})^2 + (E_4 - E_{ave})^2}{3}} \qquad (8)$$

One can get the standard deviation of PDMS network 5:1's elastic modulus of 0.11 MPa.

Figure 12. Elastic modulus of PDMS network 5:1.

From Figure 12, the elastic modulus of PDMS network 5:1 is 3.59 MPa (SD 0.11 MPa).

19

2.3.2 PDMS Network Sample 7:1

PDMS network 7:1 sample is made of 18.2 g Sylgard 184 silicone elastomer base and 2.7 g Sylgard 184 silicone elastomer curing agent. Similar to compression testing procedure of PDMS network 5:1 cylinder samples, the same procedure for PDMS network 7:1 samples was performed and the details are listed in Table 3.

Table 3. Macroscopic compression test for PDMS network 7:1.

	Sample 1	Sample 2	Sample 3	Sample 4
Thickness, mm	3.01	2.991	2.996	2.941
Diameter, mm	3.855	3.856	2.885	2.875
Diameter/Thickness Ratio	1.281	1.289	0.963	0.978
Elastic Modulus, MPa	2.950	2.924	2.867	2.894

The data of PDMS network 7:1 elastic modulus is quite repeatable. The elastic modulus of PDMS network 7:1 data are summarized in Figure 13.

Figure 13. Elastic modulus of PDMS network 7:1.

From Table 3 and Figure 13, the elastic modulus of PDMS network 7:1 is 2.91 MPa (SD 0.036 MPa).

2.3.3 PDMS Network Sample 10:1

PDMS network 10:1 is made of 18 g Sylgard 184 silicone elastomer base and 1.8 g Sylgard 184 silicone elastomer curing agent. Following the compression testing procedure of PDMS network 5:1 cylinderical samples, PDMS network 10:1 sample results are listed in Table 4.

Table 4. Macroscopic compression test for PDMS network 10:1.

	Sample 1	Sample 2	Sample 3	Sample 4
Thickness, mm	2.822	2.786	2.64	2.62
Diameter, mm	3.851	3.851	2.831	2.831
Diameter/Thickness Ratio	1.365	1.382	1.072	1.081
Elastic Modulus, MPa	2.605	2.633	2.780	2.630

Figure 14. Elastic modulus of PDMS network 10:1.

From Table 4 and Figure 14, the elastic modulus of PDMS network 10:1 is 2.66 MPa (SD 0.0797 MPa).

2.3.4 PDMS Network Sample 16.7:1

PDMS network 16.7:1 is made of 20 g Sylgard 184 silicone elastomer base and 1.2 g Sylgard 184 silicone elastomer curing agent. PDMS network 16.7:1 sample testing results are listed in Table 5.

Table 5. Macroscopic compression test for PDMS network 16.7:1.

	Sample 1	Sample 2	Sample 3	Sample 4
Thickness, mm	2.515	2.493	2.502	2.517
Diameter, mm	3.803	3.8	2.666	2.708
Diameter/Thickness Ratio	1.512	1.524	1.065	1.076
Elastic Modulus, MPa	1.109	1.234	1.265	1.227
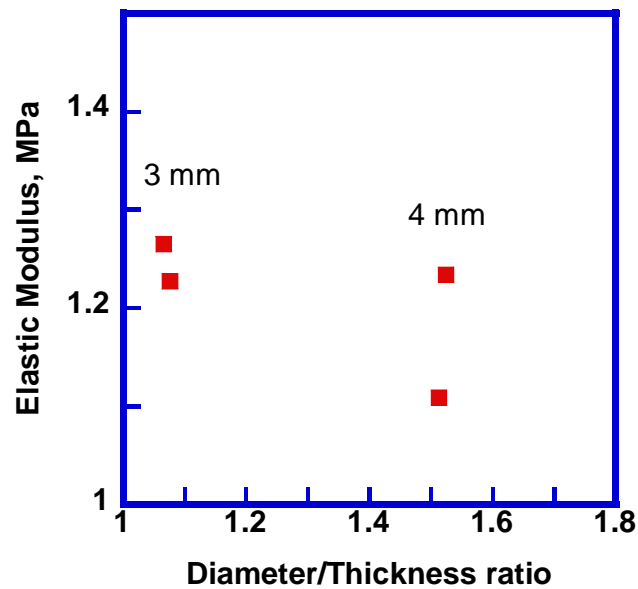
Figure 15. Elastic modulus of PDMS network 16.7:1.

From Table 5 and Figure 15, elastic modulus of PDMS network 16.7:1 is 1.21 MPa (SD 0.069 MPa).

2.3.5 PDMS Network Sample 25:1

PDMS network 25:1 is made by 30.5 g Sylgard 184 silicone elastomer base and 1.2 g Sylgard 184 silicone elastomer curing agent. PDMS network 25:1 sample macroscopic compression testing results are listed in Table 6.

Table 6. Macroscopic compression test for PDMS network 25:1.

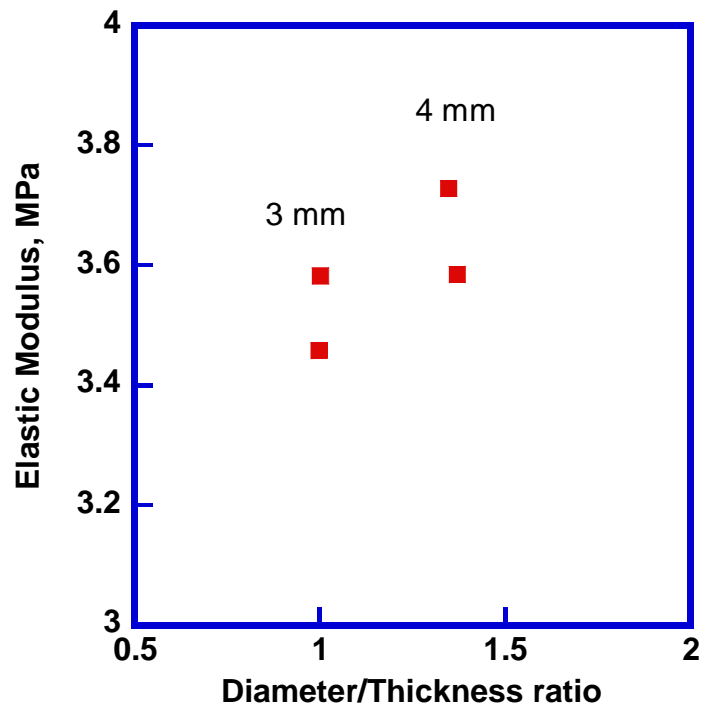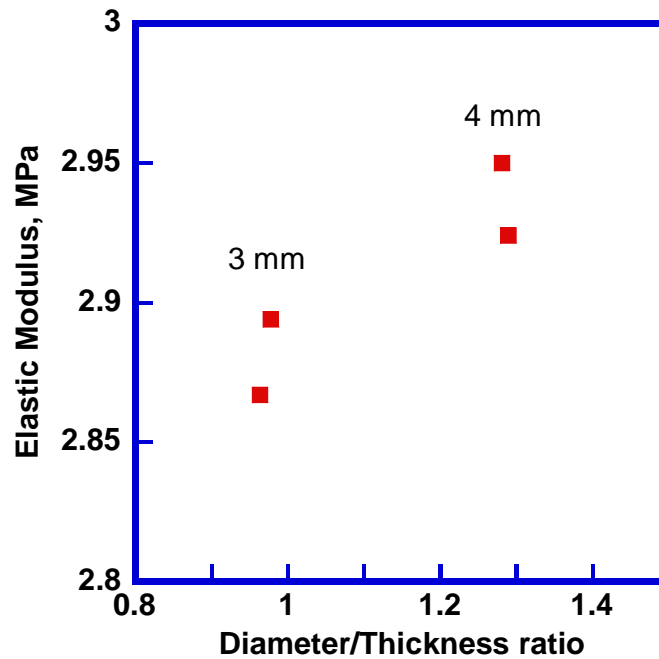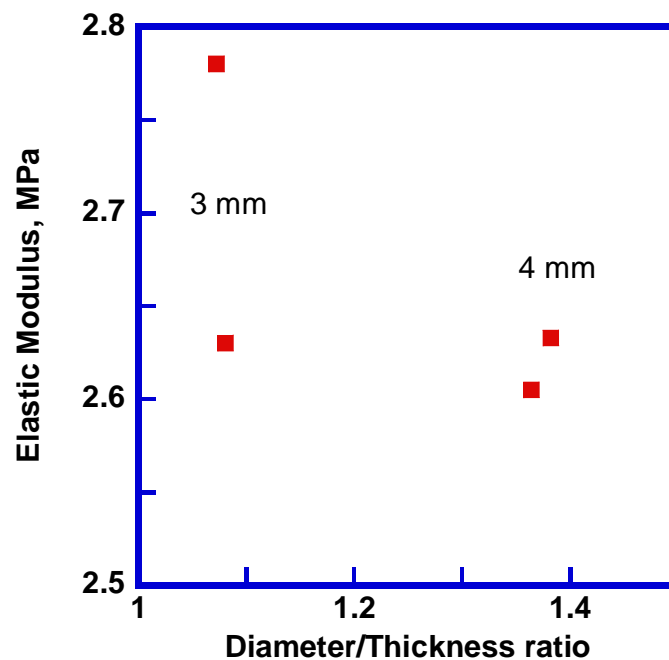|	Sample 1	Sample 2
Thickness, mm	2.428	2.403
Diameter, mm	3.652	2.665
Diameter/Thickness Ratio	1.504	1.109
Elastic Modulus, MPa	0.954	1.006
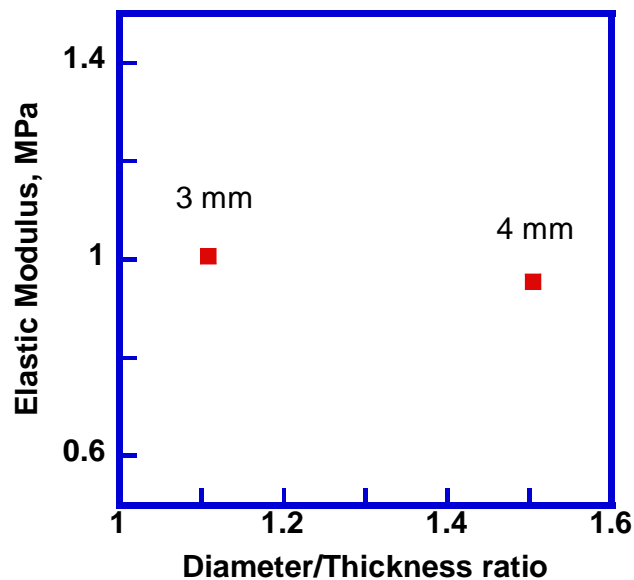
Figure 16. Elastic modulus of PDMS network 25:1.

From Table 6 and Figure 16, the elastic modulus of PDMS network 25:1 is 0.98 MPa (SD 0.0368 MPa).

2.3.6 PDMS Network Sample 33:1

PDMS network 33:1 is made of 19.5 g Sylgard 184 silicone elastomer base and 0.59 g Sylgard 184 silicone elastomer curing agent. PDMS network 33:1 sample testing results are listed in Table 7. PDMS network 33:1 elastic modulus is 0.56 MPa (SD 0.021 MPa).

Table 7. Macroscopic compression test for PDMS network 33:1.

	Sample 1	Sample 2
Thickness, mm	2.435	2.435
Diameter, mm	3.380	3.380
Diameter/Thickness Ratio	1.388	1.388
Elastic Modulus, MPa	0.548	0.577

2.4 Conclusions of Chapter 2

The elastic modulus results (Table 8) based on the macroscopic compression tests show that PDMS's elastic modulus is related to the samples' base/agent ratio (the degrees of crosslinking). The relationship between PDMS network elastic modulus and its base/agent ratio is studied in the following. [22-26]

Table 8. Elastic modulus of PDMS network.

	E_1, MPa	E_2, MPa	E_3, MPa	E_4, MPa	E_{ave}, MPa
	Diameter around 4mm		Diameter around 3mm		
PDMS 5:1	3.584	3.728	3.458	3.582	3.59
PDMS 7:1	2.950	2.924	2.867	2.894	2.91
PDMS 10:1	2.605	2.633	2.780	2.630	2.66
PDMS 16.7:1	1.109	1.234	1.265	1.227	1.21
PDMS 25:1	0.954	-	1.006	-	0.98
PDMS 33:1	0.548	0.577	-	-	0.56

24

2.4.1 PDMS Modulus' Dependence on the Base/Agent Ratio

Different curve fittings are done to describe the relationship between the modulus of PDMS network and its base/agent ratio.

1. Logarithmic Curve Fitting

Exponential curve fitting is also done to describe the relationship between Elastic Modulus and PDMS network base/agent ratio, which is shown in figure 17 and written as:

$$E = 6.214 - 3.8034 \log(n), \quad R = 0.98286. \tag{9}$$

E is PDMS's elastic modulus, and n is PDMS network base/agent ratio.
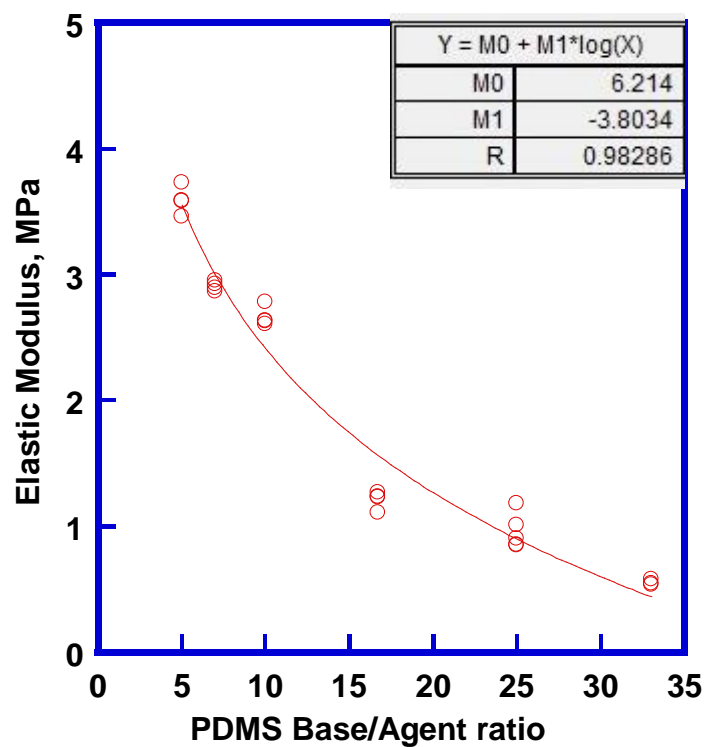
Figure 17. Logarithmic curve fitting of PDMS network elastic modulus.

25

2. Polynomial Curve Fitting

Polynomial curve fitting is done to describe the relationship between Elastic Modulus and PDMS network Base/Agent ratio, which is shown in figure 18 and written as:

$$E=4.7345-0.26896*n+0.0044*n^2, R=0.98455. \qquad (10)$$

E is PDMS's elastic modulus, and n is PDMS network base/agent ratio.
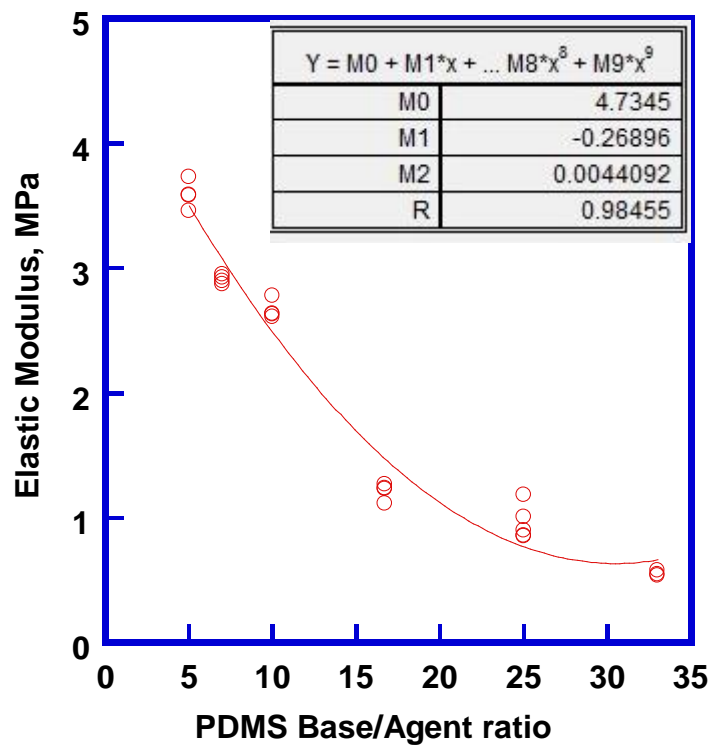
Figure 18. Polynomial curve fitting of PDMS network elastic modulus.

26

3. Exponential Curve Fitting

Exponential curve fitting is also done to describe the relationship between Elastic Modulus and PDMS network Base/Agent ratio, which is shown in Figure 19 and written as:

$$E = 4.699e^{-0.066326n}, R = 0.98372. \tag{11}$$

E is PDMS's elastic modulus, and n is PDMS network base/agent ratio.
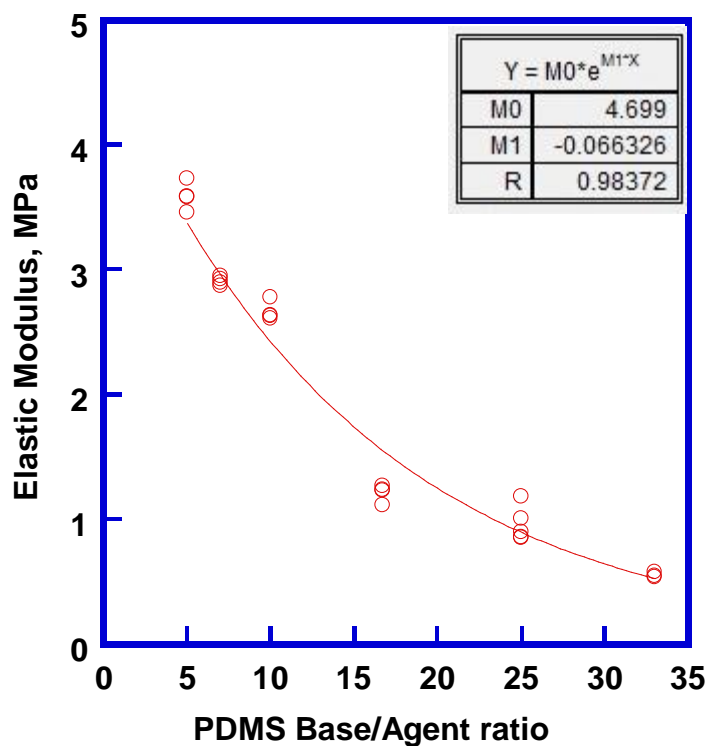
Figure 19. Exponential curve fitting of PDMS network elastic modulus.

4. 1/x Curve Fitting

In Figure 17, reverse function curve fitting is done to describe the relationship between PDMS network elastic modulus and its base/agent ratios, which can be written as:

$$E=19.981/n, R=0.95266 \qquad (12)$$

where, E is PDMS's elastic modulus, and n is PDMS network base/agent ratio.
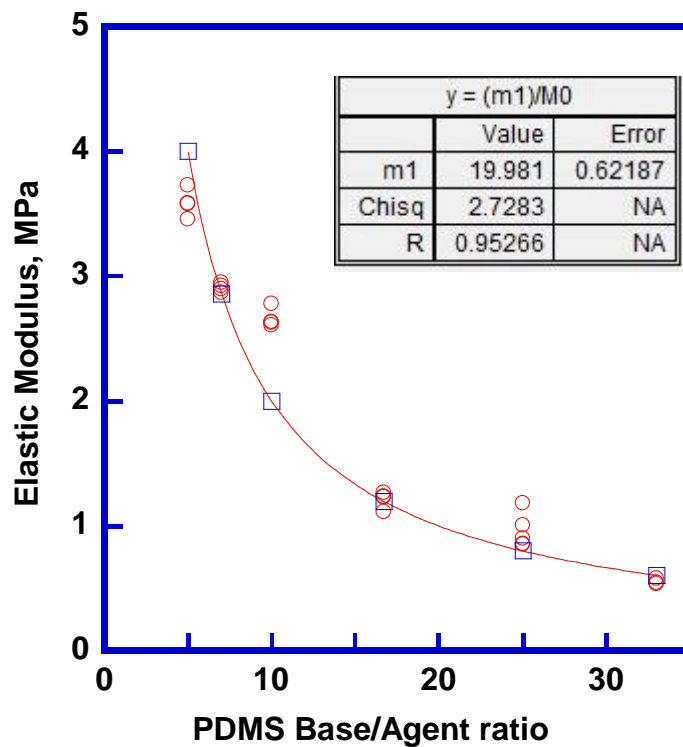
Figure 20. 1/x curve fitting of PDMS network elastic modulus.

In equation 12, it is easy to see 1/n is agent/base ratio, which is also the amount of crosslinker in PDMS network sample. So it means the PDMS network elastic modulus is linear with its amount of crosslinker.

Overall, comparing with R values of these curve fittings, they are all very close to each other. The polynomial curve fitting maybe a better fit according to its R value: $E=4.7345-0.26896*n+0.0044*n^2$.

28

However, the reverse founction curve fitting has physical meaning. Except for the amount of crosslinker(PDMS network cure agent), all other experiment conditions are the same for each PDMS network sample test. Therefore, the PDMS network elastic modulus is linear with its percent of crosslinker.

2.4.2 PDMS Network Modulus' Dependence on the Samples' Diameter/Length Ratio

The ratio between the initial length L_0 and the diameter D of the sample is a pertinent parameter. In this macroscopic compression test, all the cylindrical samples lengths are around 3mm, but the diameters are varying with two sizes: 3mm and 4mm. The affect of sample's diameter for its elastic modulus are shown in Figure 21.
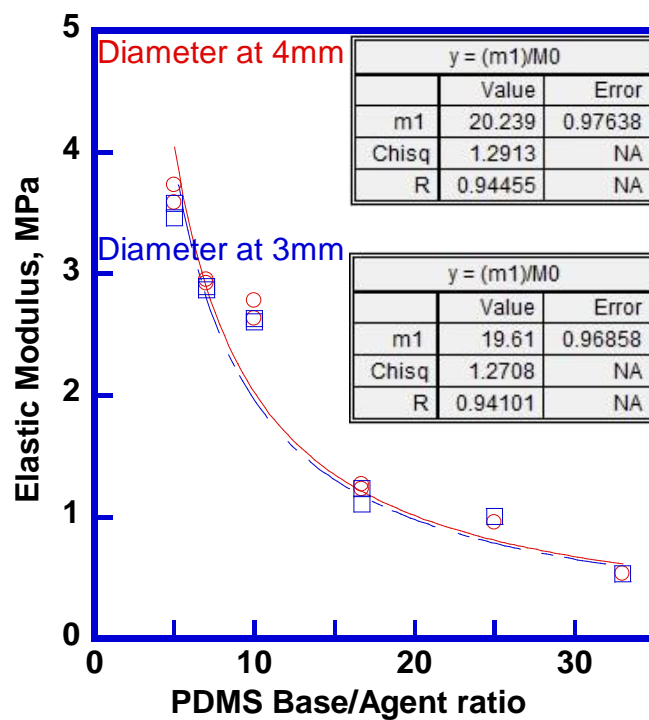
Figure 21. 1/x curve fitting of PDMS network elastic modulus with diameter

at 3 and 4 mm.

29

In Figure 21, elastic moduli of samples with diameter at 4mm are plotted in red and elastic moduli of samples with diameter at 3mm are plotted in blue. It shows the diameter of sample does not really affect the PDMS's elastic modulus.

2.4.3 Effect of Friction on PDMS Network Modulus

There are different deformation modes in compression testing, for example: buckling, shearing, barreling, homogenous compression. When barreling happens, friction is present at the contact surface. [27] In this compression test, the deformation mode is barreling, so additional compression experiments with oil are done to discuss the friction effect on PDMS network modulus. The data are shown in Table 9.

Table 9. Effect of friction on PDMS network modulus

	E_1, MPa	E_2, MPa	E_3, MPa	E_4, MPa
	Without oil		Oil test	
PDMS 5:1	3.584	3.728	3.54	3.57
PDMS 7:1	2.950	2.924	2.87	2.91
PDMS 10:1	2.605	2.633	2.48	2.55
PDMS 16.7:1	1.109	1.234	1.361	1.276
PDMS 25:1	0.954		0.883	0.881
PDMS 33:1	0.548	0.577	0.489	
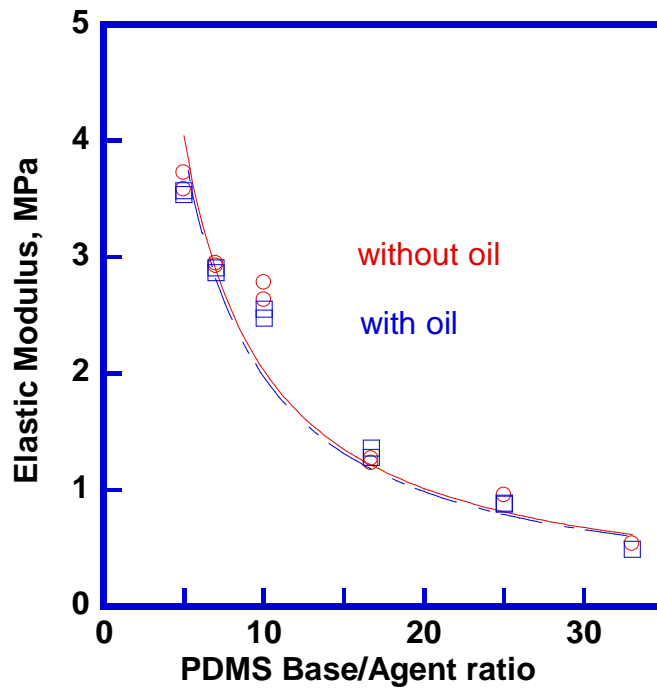
Figure 22. Friction does not affect PDMS network elastic modulus

In Table 9 and Figure 22, it is clear that the elastic modulus of PDMS network reduces in compression testing with oil, which means there is friction happening during the test. But comparing with the stress applied on sample during the test, the friction is not a big effect of the compression test. Also, the reverse function curve fitting does not change much no matter whether there is friction.

One may notice that the elastic modulus of PDMS network 16.7:1 in compression oil test is bigger than the data in compression without oil test. That is because the initial force in PDMS network 16.7:1 compression without oil test is 20 g, but the initial force in other samples' tests are 50 g. Without enough preload before the compression test, the elastic modulus of sample will be smaller than its true value. This is another example of the necessary of pre-loading method in this research.

31

Chapter 3. Nanoindentation of PDMS

3.1 Introduction to Nanoindentation

Another method used to characterize materials' mechanical properties is the nanoindentation test. Nanoindentation technology is widely and efficiently used to test sensitive surface forces and mechanical properties of thin films and MEMS devices [27-30]. Hysitron Triboindenter is one of the commonly used nanoindentation machines, which is shown in Figure 23.

Figure 23. Hysitron Triboindenter.

The main parts of Hysitron Triboindenter consist of a tandem piezoelectric ceramic scanning tube and a transducer. The piezoelectric ceramic tube can provide very fine positioning of the indenter tip during testing. The transducer is the heart of the nanoindenter which records force/displacement data [9]. Figure 24 shows the cross-section of a center plate capacitor transducer. When a voltage is applied to the drive plates, it produces an electrostatic attraction between the spring loaded center plate and the bottom plate, and causes the center plate to move making an indent [9].
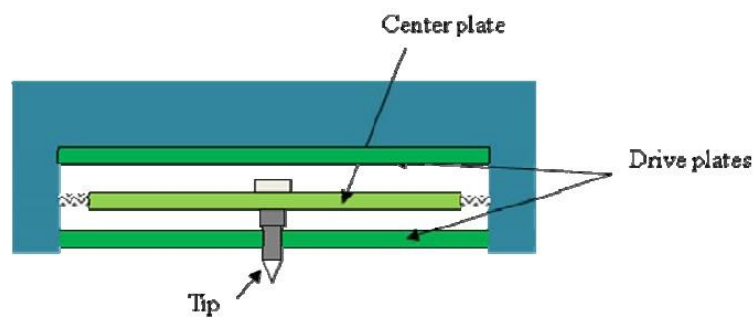
Figure 24. Transducer cross section of Hysitron Triboindenter [9].

In nanoindentation test, a tip penetrates into the sample and the load-displacement curve is recorded. In this process, the compliances of the machine, the indenter tip and the sample are also recorded. The relationship can be described as in [9]:

$$C=C_m+C_1 \tag{13},$$

where C is the measured compliance, C_m is the machine compliance and C_1 is the response of indenter and sample. From this relationship, C_1 is then used to derive the reduced modulus. The accuracy of the reduced modulus is highly dependent on the value of C_m and therefore it is advised that machine compliance is tested before data are collected. The machine compliance calibration is done by testing several indents on quartz, whose hardness and reduced modulus are constant at large indentation

33

depths, and graphing of 1/measured stiffness vs. $1/P_{max}^{1/2}$ for the indentations. If it is calibrated, this should yield a straight line where y intercepts defined as the machine compliance [30]. Since PDMS network is quite soft, machine compliance effects do not affect the modulus measurements as much as for stiffer materials.

3.2 Samples Preparation

PDMS network was polymerized by the same method discussed in chapter 2 but the sample preparation was altered to accommodate the nanoindention workspace. In this instance samples were prepared as 1 cm^2 pads of approximately 3 mm thickness, rather than using cylindrical punches, and are shown in Figure 25.
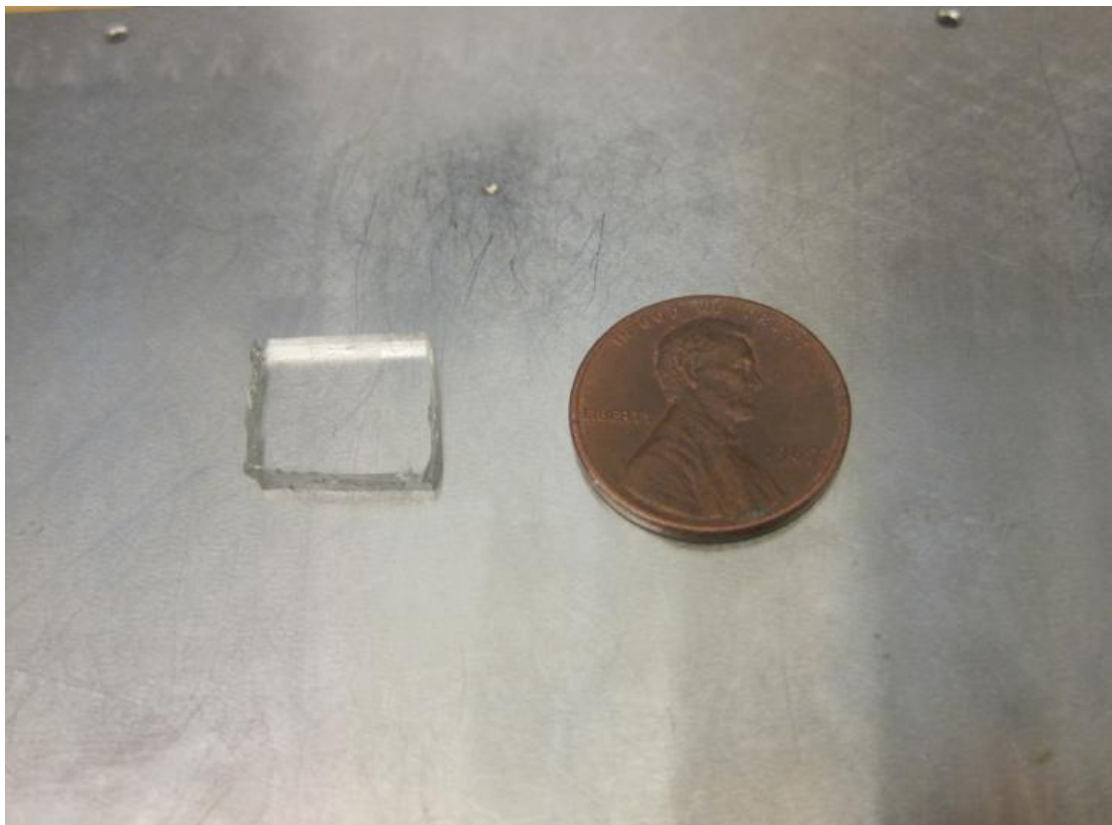
Figure 25. Sample for nanoindentation.

3.3 Experiments and Data for Nanoindentation Tests

For nanoindentaion tests, different models are used to test different materials. Quasi-static test can be used to study the mechanical properties of metallic thin films. DMA system can be used to test the complex modulus of soft polymers. Also, different experimental conditions and different methods are used to achieve the valuable results.

3.3.1 Dynamic Mechanical Analysis

The dynamic mechanical analysis (DMA) system is used for the test. DMA nanoindentation is a well developed procedure of Hysitron Triboindenter. It is convenient to get the complex modulus of PDMS network with DMA nanoindentation test [9], which is different from conventional DMA test. To conventional DMA testing, the instrument is complicated to control and the testing process depends too much on the testing temperature.

There are different control models in DMA systems, specifically, frequency control, dynamic force control and static force control. For time-dependent behavior, dynamic viscoelastic testing offers the advantage of significantly decreased testing time by examining properties over a range of frequencies rather than extended time. [31-33]

The equations for DMA method calculation are:

$$E^{'} = \frac{k_s \sqrt{\pi}}{2\sqrt{A}} , \quad E^{"} = \frac{\omega C_s \sqrt{\pi}}{2\sqrt{A}} \tag{14},$$

where k_s is the storage stiffness of the sample, C_s is the loss stiffness of the sample, A is the contact area. Transducer is calibrated before the data are collected, shown in the Figure 26.

35
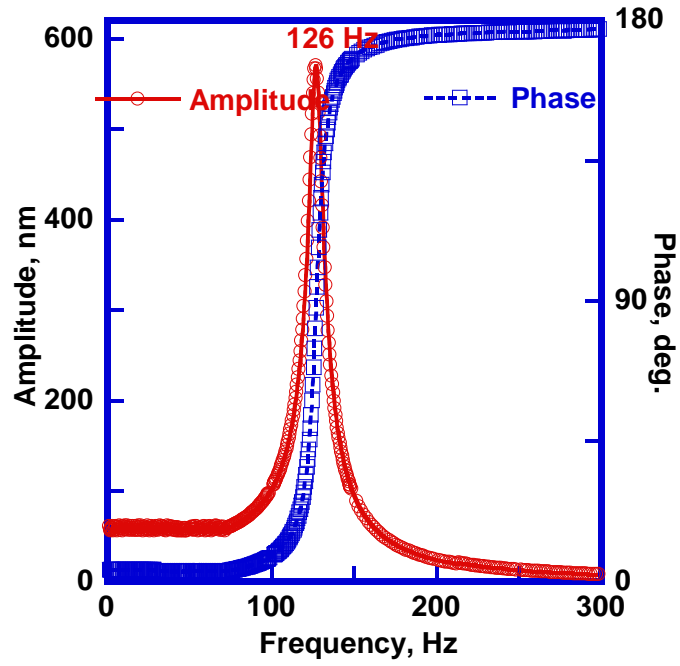
Figure 26. Transducer calibration.

After proper calibration, transducer mass was determined at 260.23 mg, the center plate spring constant k_i is 166.73 N/m, damping C_i is 0.0141 kg/sec, and the transducer resonance frequency is 126 Hz.

36
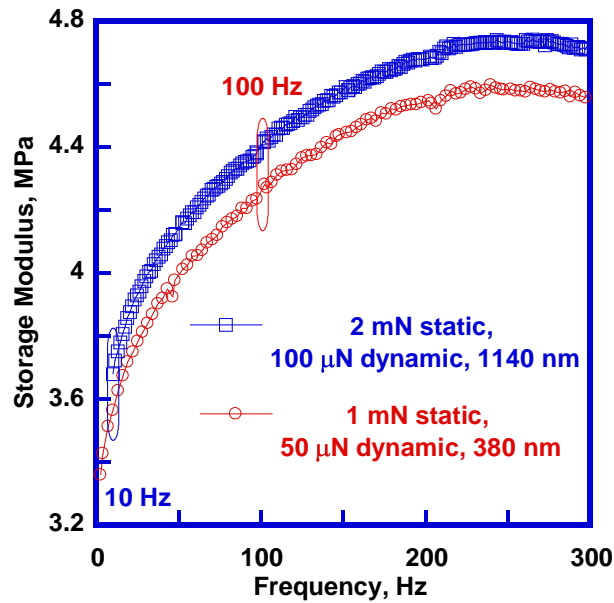
Figure 27.a. Storage modulus from the frequency sweep DMA test for

PDMS network 5:1.

With the test data file, one can get storage and loss stiffness of the sample, and using equations 14 to calculate the storage modulus and loss modulus. Figure 27.a shows the storage modulus of PDMS network 5:1 in DMA frequency control test. PDMS's storage modulus is increasing when the frequency. Also, at low frequency, the DMA result is similar to the flat punch quasi-static test. In Figure 27.a, it is easy to see PDMS network 5:1's storage modulus is around 3.5 MPa when the frequency is at 10 Hz with the nanoindentation depth at 380 nm, which is comparable to the PDMS 5:1 compression test data. The PDMS network 5:1's storage modulus is around 4.4 MPa when the frequency is at 100 Hz and with the nanoindentation depth at 1140 nm.

37
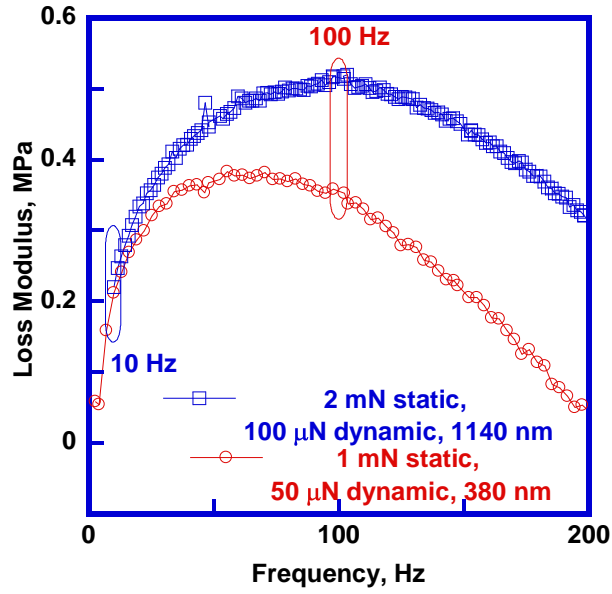
Figure 27.b. Loss modulus from the frequency sweep DMA test for

PDMS network 5:1.

Figure 27.b shows the loss modulus of PDMS network 5:1 in DMA frequency control test. PDMS's loss modulus is changing with test frequency. In figure 27.b, one can see the loss modulus reaches the peak when the test frequency gets close to the transducer's resonance frequency.
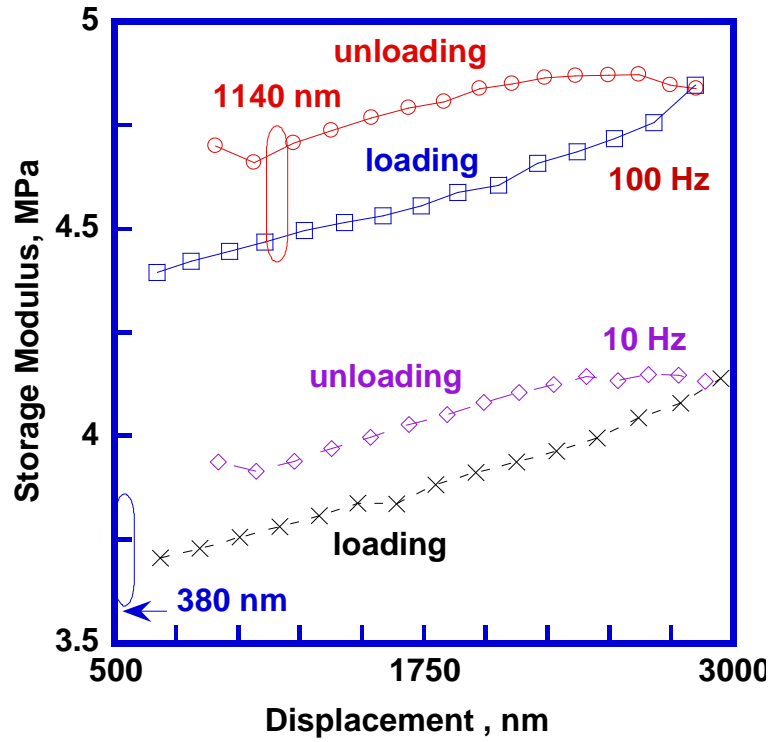
Figure 28.a. Storage modulus of PDMS network 5:1 in the force control test.
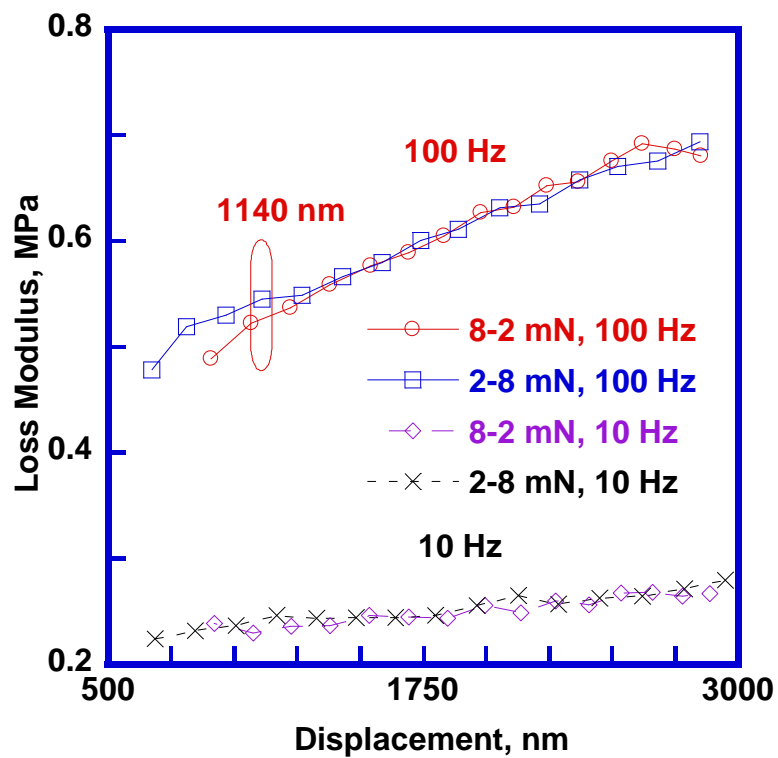
Figure 28.b. Loss modulus of PDMS network 5:1 in the force control test.

39

Figure 28.a shows the storage modulus of PDMS network 5:1 in DMA static force control test. Static force is set from 2 mN to 8 mN, dynamic force is set at 50 μN, frequency is set at 10 Hz and 100 Hz, respectively. The difference between PDMS network loading and unloading tests is due to the viscoelastic properties of PDMS. In Figure 28.a, storage modulus of PDMS network 5:1 at 1140 nm nanoindentation depth is around 4.5 MPa, which is comparable to the data shown in Figure 27.a. Also, storage modulus of PDMS network 5:1 at 380 nm nanoindentation depth with 10 Hz test frequency is around 3.5 MPa, which is the same with the data shown in Figure 27.a and the PDMS network 5:1 elastic modulus from compression test.

Figure 28.b shows the loss modulus of PDMS network 5:1 in DMA static force control test, which is similar to experiments shown in Figure 27.b. The loss modulus of PDMS network is stable whether in loading or unloading tests. The loss modulus of PDMS network 5:1 in Figure 28.a at 1140 nanoindentation depth and with 100 Hz test frequency is similar with the data collected at the same experimental conditions as in Figure 27.a.

Thus, PDMS network nono-DMA test provides stable data with different test control models. Also the elastic modulus collected in nano-DMA test is comparable with the data collected in PDMS network compression test for PDMS network 5:1 sample.

3.3.2 PDMS Network Nanoindentation Test with Flat Punch Tip

A flat punch tip (MS02091001) was used in PDMS's nanoindentation tests. It has a cylindrical shape and the diameter is 1002.19 μm. Because soft material like PDMS network is not as stiff as metals, several hundred times bigger depth of PDMS network nanoindentation will be produced with the same load. However, this problem will be avoided when a flat punch tip is used in experiments [34, 35].

The commonly used method for calculating mechanical properties of materials is the Oliver-Pharr method and it is also appropriate for flat punch nanoindentation test. In this continuous stiffness method, the upper unloading curve is used [9, 30]:

$$S = \frac{dP}{dh} \tag{15},$$

$$P = q(\delta - \delta_{pl})^m \tag{16},$$

where S is the slope of upper unloading curve, q and m are the fitting parameters, P is the maximum load in an indentation test and δ is the indentation depth determined from the unloading curve.

The contact depth is written by:

$$h_c = h_t - w\frac{P}{dP/dh} \tag{17},$$

where h_t is the total indentation depth, w is an indenter geometry factor.

The reduced modulus can be calculated from:

$$S = \beta\frac{2}{\pi}E_r\sqrt{A_C} \tag{18},$$

where A_C is the contact area and β is an indenter shape constant.

With known β, the reduced modulus of the sample in equation 18 thus can be changed as:

41

$$E_r = \frac{S\sqrt{\pi}}{2\sqrt{A}} \qquad (19),$$

For the perfect Berkovich tip, the tip area A=24.5 depth^2, but for the flat punch used in this research, the diameter of the tip is known at 1002.19 μm, therefore, the equation 19 can be simplified as,

$$E_r = \frac{S\sqrt{\pi}}{2\sqrt{A}} \longrightarrow \frac{S}{2R} = \frac{S(\mu N / nm)}{D(1002.19\mu m)} = \frac{S}{1.00219}(MPa) \qquad (20),$$

From the upper part of the unloading curve, one can get S(slope) in equation 20, then the reduced modulus can be calculated accordingly.

PDMS network 5:1 sample, 1.65 mm thick was used for the flat punch experiments. The sample was placed on the steel substrate to avoid any air bubbles between the sample and substrate.
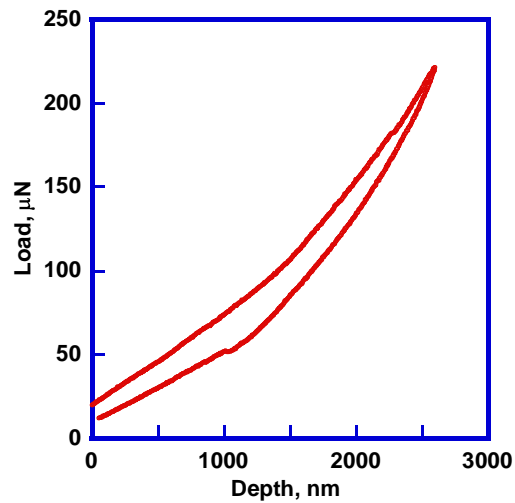
Figure 29. PDMS network 5:1 nanoindentation with flat punch tip.

Based on equation 20, since the elastic modulus of PDMS network is constant, the slope of nanoindentation load-displacement curve should also be constant, but the slope in Figure 29 is changing. This happens due to incomplete contact between the

42

cylinder tip and the sample misalignment. The flat punch tip has a large diameter of 1002.19 µm, and when it touches the sample, the initial contact does not involve the whole surface area of the flat tip as shown schematically in Figure 30.
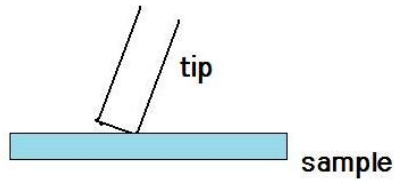
Figure 30. The initial contact of PDMS network during flat punch nanoindentation test showing partial contact.

To solve this problem, preload method was used to perfrom the flat punch nanoindentation test. In the imaging window of the Hysitron software the sample was moved into the tip in 5 µm increments, for the 40 µm total displacement. More details are shown in Figure 31.

43
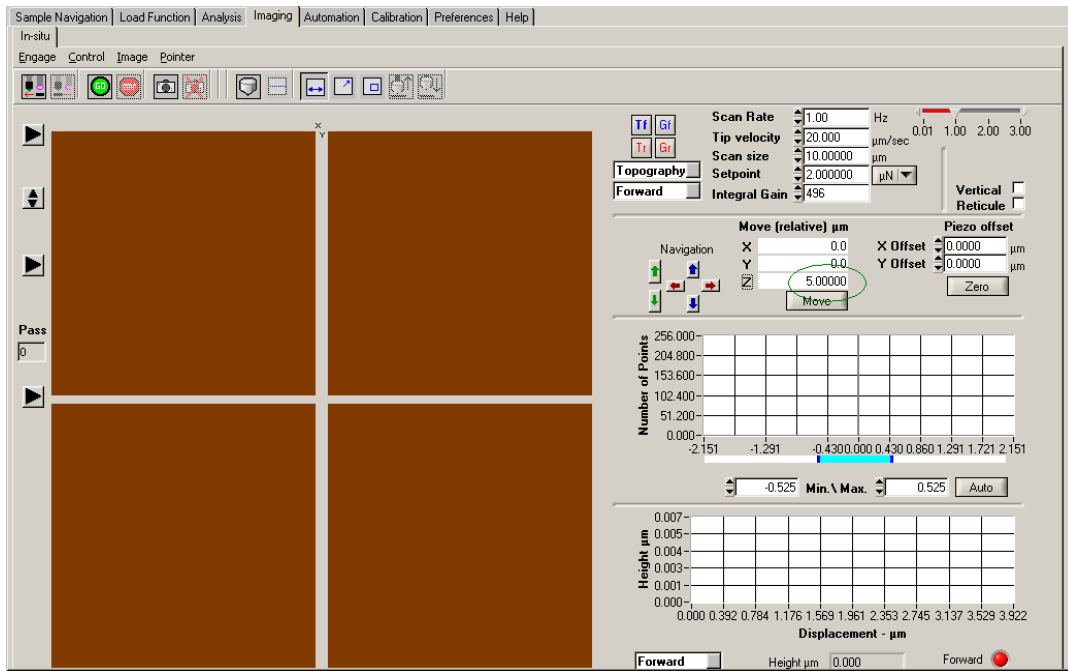
Figure 31. The set up of pre-load flat punch tip nanoindentation test.

After 40 μm total displacement into the sample, the load changes linearly, which means that the tip and the sample developed full contact. After this pre-loading procedure one can start an indent. The preload flat punch tip nanoindentation test is shown in Figure 32. Different experiments with different load functions and different drift monitor times are also done in this section.
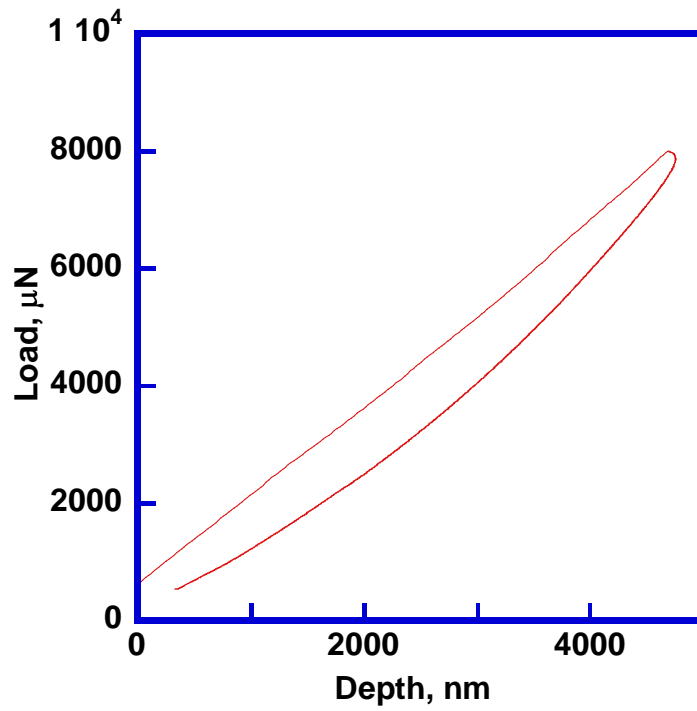
Figure 32. Flat punch nanoindentation of PDMS network 5:1.
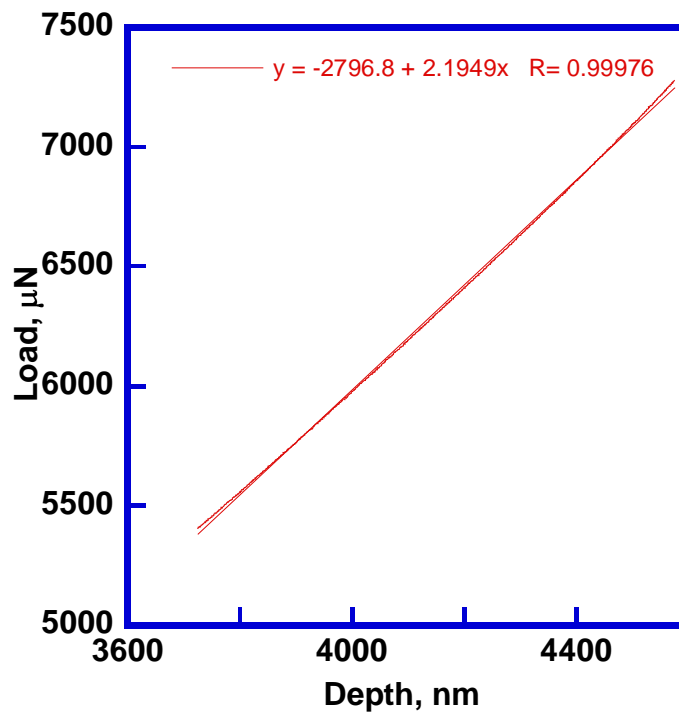
Figure 33. Linear fitting for upper unloading of nanoindentation curve in Figure 32.

45

Typical nanoindentation curve is shown in Figure 32. Linear fitting is made for the upper unloading curve, which is shown in Figure 33. According to equation 20, the elastic modulus of PDMS network 5:1 is 2.2 MPa.

This value of PDMS network 5:1 elastic modulus in flat punch Quasi test is lower than the data from DMA test and compression test. The reason is because pre-loading 40 µm maybe not enough.

There is no voltage applied to the transducer in this pre-loading process, so the transducer spring will move backwards due to the pushing back force yielded when the tip is pushing the sample. To PDMS network, its elastic property can be described using spring model. In this case, the pre-loading procedure can be explained with two-spring model, which is shown in Figure 34.

Transducer with spring
constant 167 N/m

40 µm displacement, 1
mm diameter flat punch

Sample with spring
constant y 3500 N/m
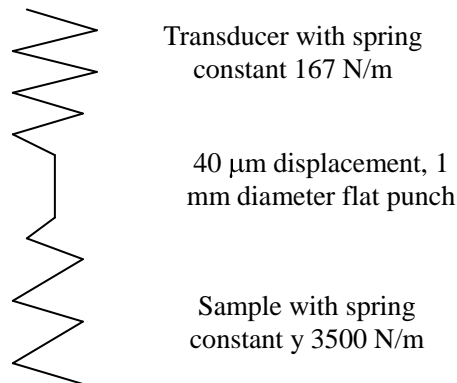
Figure 34. Two-spring model for the transducer and the sample.

In DMA nanoindentation, one can get the transducer spring constant is 167 N/m and the PDMS network 5:1 sample's stiffness is 3.5 µN/nm. It is easy to see the stiffness of the sample is around 20 times of the stiffness of transducer's spring. So when 40µm displacement happens during pre-loading process in Figure 34, the

46

displacement of flat punch moving towards the sample is 2 μm. In the case the flat punch's diameter is 1002.19 μm, the misalignment angle of the flat punch is 0.12°. Therefore, to this flat punch Quasi test, the elastic modulus of PDMS network 5:1 is 2 times different from the data in DMA nanoindentation and macroscopic compression test, it is possible the test is still not developing full contact.

The same experiments performed with different unloading rates are shown in Figure 35.a and Figure 36.
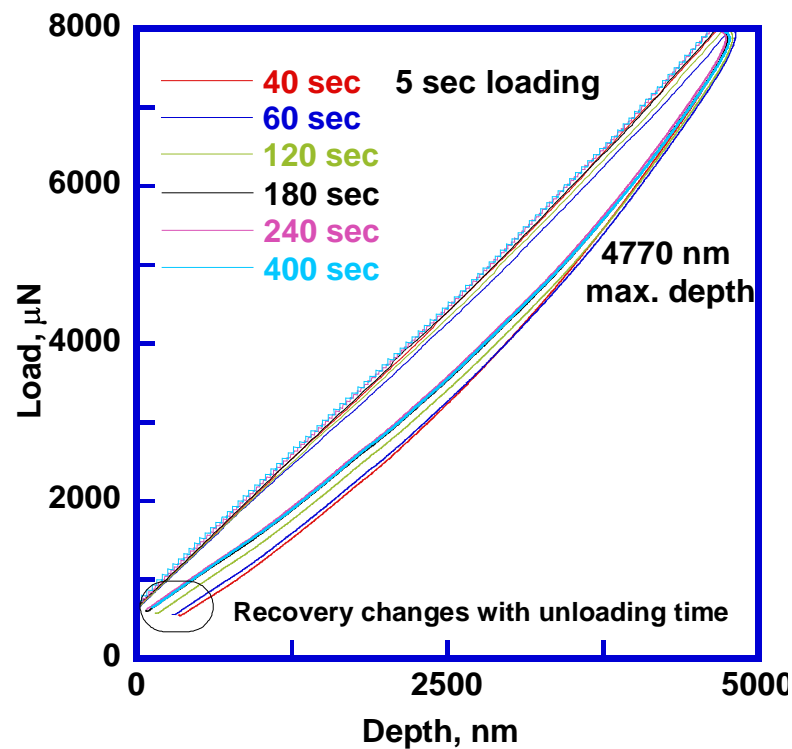
Figure 35.a. PDMS network 5:1 nanoindentation recovery behavior.
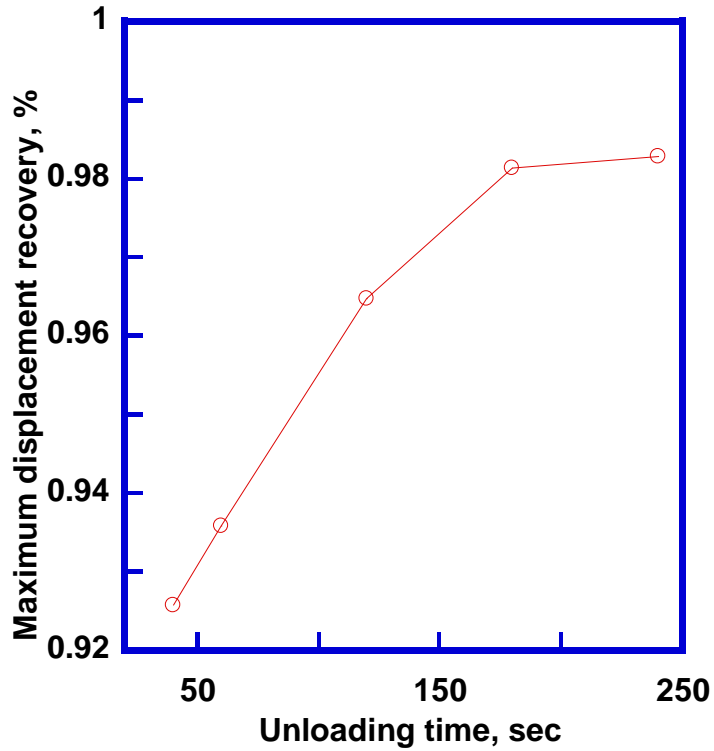
Figure 35.b. PDMS network 5:1 nanoindentation recovery-time relationship.

Because of PDMS polymer's viscoelastic properties, creep happened during the PDMS network's loading procedure, the creep recovered when unloading process started, and PDMS's nanoindentation recovery behavior depends on the unloading rate [1, 20]. Figure 35.b shows the quantitative relationship between PDMS network nanoindentation recovery and the unloading rate. [1, 39-41] One can see that the samples' recovery will complete if a long enough unloading time is applied.
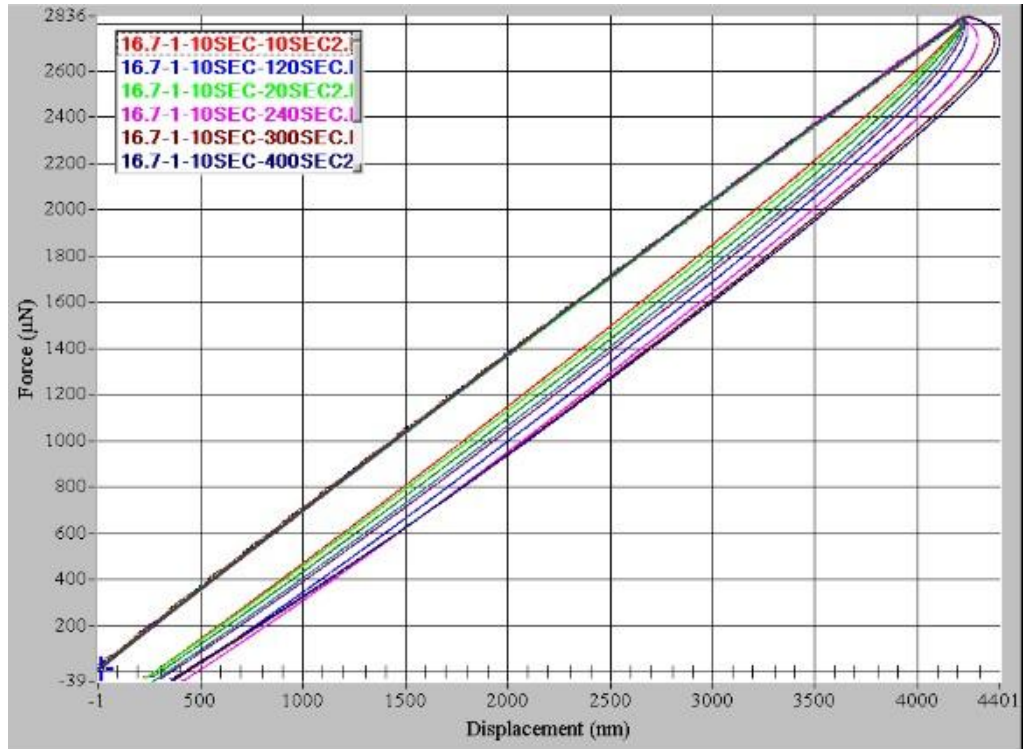
Figure 36. PDMS network 16.7:1 nanoindentation recovery-time relationship.

3.3.3 Adhesion Force -- Berkovich Tip

The Berkovich tip has three sides with a total included angle of 142.35°, and is one of the most commonly used tips [9, 42-44]. It is also the standard tip used in nanoindentation tests [9]. Berkovich tips are made of diamond with a modulus of 1140 GPa.

49
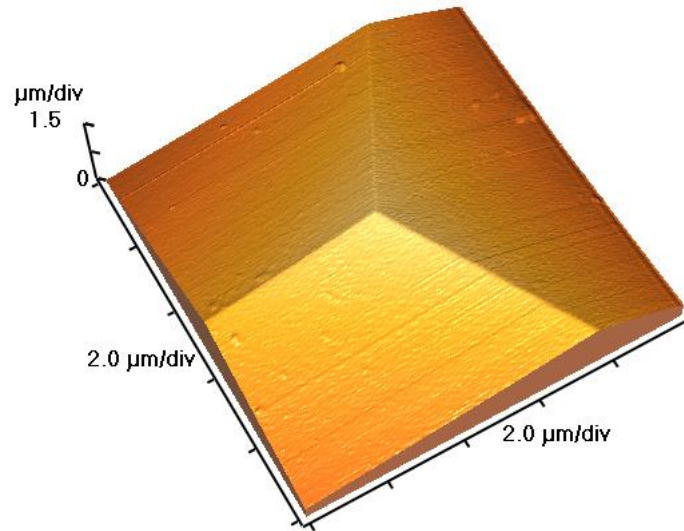
Figure 37. The Berkovich tip AFM geometry image.

Because of the versatility of the Berkovich tip it seems it is a natural candidate for testing the properties of PDMS. However, the testing process has some interesting phenomena which have never been seen in other materials tests. The Berkovich PDMS network nanoindentation test is shown in Figure 38. PDMS network is soft (E < 5 MPa), so when the sharp Berkovich tip is approaching the surface of the sample, it is difficult for the transducer to determine the initial contact point. Conversely, when the tip is withdrawing from the sample's surface, surfaces adhesion forces make it difficult to predict the sample's surface [45, 46].

The transducer is calibrated before the experiments. The surface is detected by approaching the sample and touching its surface with 2 μN force. This method does not work for PDMS network because even at 2 μN force the tip is already indenting the sample. An alternative method was used where the Berkovich tip is brought close to the surface (~1.5 μm) before the test is started.   This is done because the initial

50

contact will be shown clearly when the tip is contacting the sample. The resulting data
curve may be found in Figure 38 below.
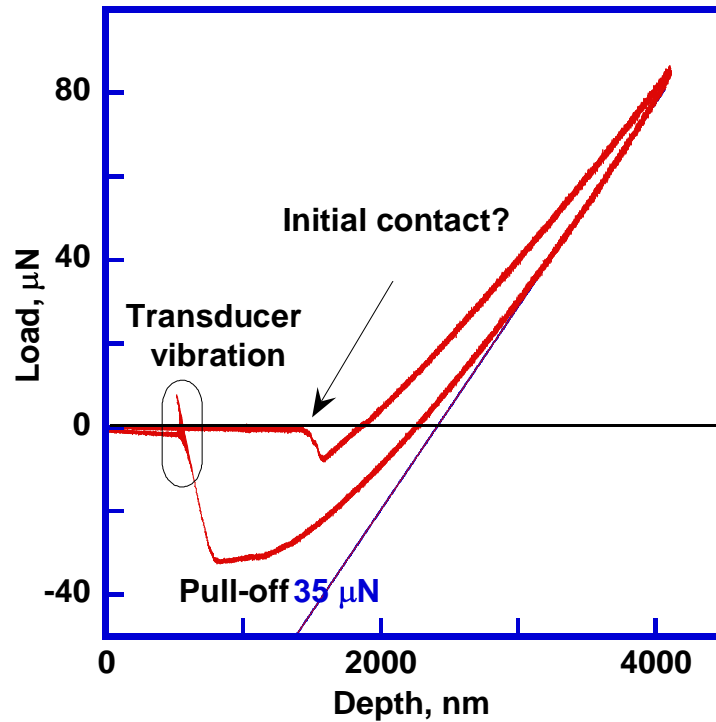
Figure 38. Berkovich tip nanoindentation test of PDMS network 5:1.

In Figure 38, the tip touches the sample's surface after traveling the last 1.5µm in
air. The pull-in negative force is present at 500 nm depth, which will affect the elastic
modulus calculation using equation 19. In Berkovich tip nanoindentation test,
Oliver-Pharr method is commonly used to generate the equation 19, which shows that
elastic modulus of the sample is related to the contact area, while the contact area for
the perfect Berkovich tip is $A=24.5$ depth^2. So because of the 500 nm depth associate
with the pull-in phenomenon, Berkovich tip is not a good choice for PDMS network
nanoindentation test without accounting for the pull-in effect.   After the pull-in

51

phenomenon, the nanoindentation load starts to increase as the tip pushes against the sample surface.

After the indentation process is done, the tip withdraws from the sample's surface. When the tip is leaving the sample surface, transducer vibration occurs. Figure 39 graphs nanoindentation load and depth over time, and the transducer's vibration can be clearly seen in more detail. One can easily see that the transducer's vibration frequency is 125 Hz, which is similar to the transducer resonance frequency of 126 Hz shown in Figure 26.
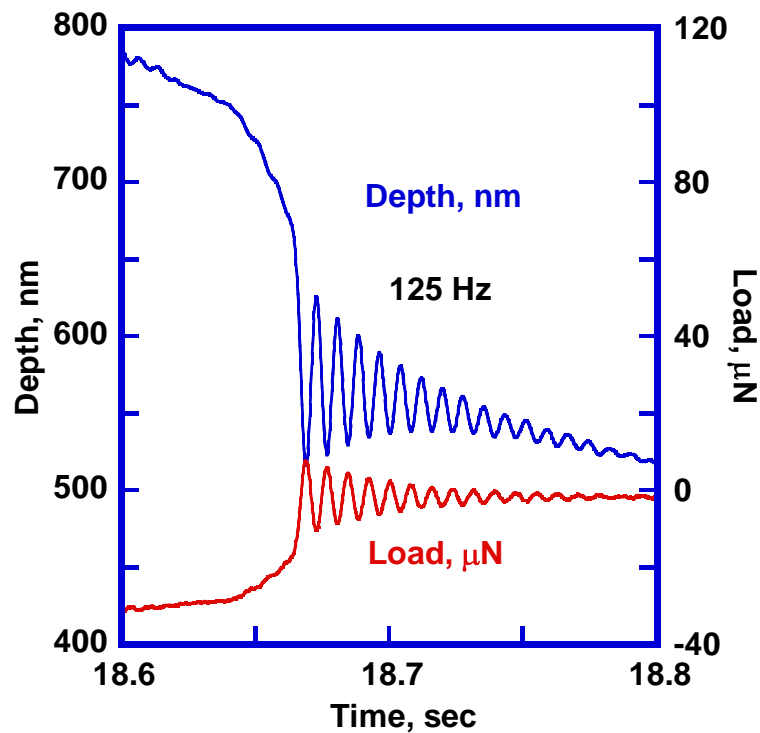
Figure 39. Transducer spring vibration.

Although the Berkovich tip nanoindentation test is not suitable for PDMS network mechanical properties research, it is functional to find the relationship between the adhesion force and the PDMS network stiffness and to study the PDMS network

52

samples' surface energy. More PDMS network samples with different base/agent ratios were tested with Berkovich tip to collect the adhesion forces and details are shown in Figure 40. Pull-off forces are present in all samples, but for these PDMS network samples with different base/agent ratios, the pull-off forces are different. The pull-off force increases with PDMS network base/agent ratio. However, the pull-off force magnitude is not as large as in Figure 38. The possible reasons why the pull-off force in Figure 40 is several times smaller than in Figure 38 is because the samples' surface in Figure 40 is not clean or the Berkovich tip used in the tests in Figure 40 is worn.
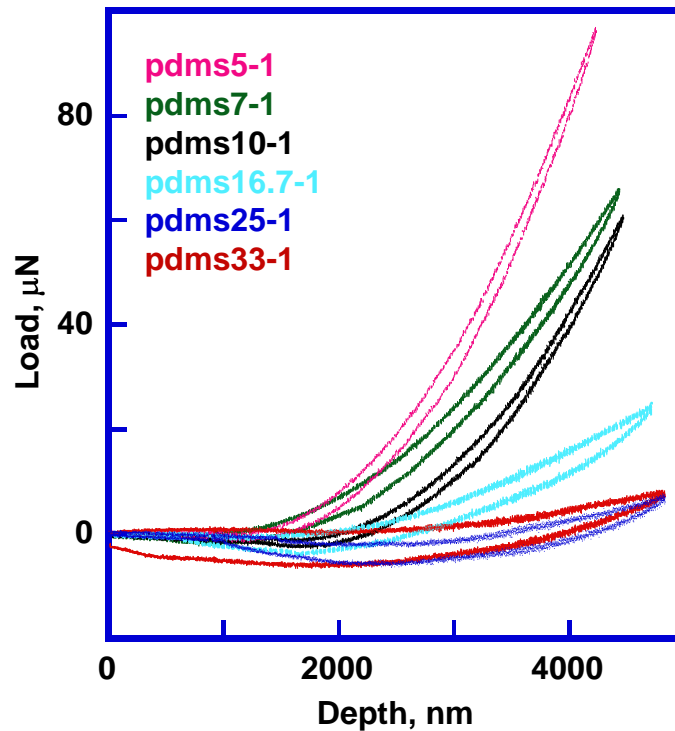
Figure 40. PDMS network samples nanoindentation tests for the pull-off forces determination.

Pull-off force of PDMS network samples determined from load-displacement curves in Figure 40 is plotted in Figure 41. The pull-off force is related to the geometric shape of the Berkovich tip, its contact area, and adhesion of PDMS network samples [47].
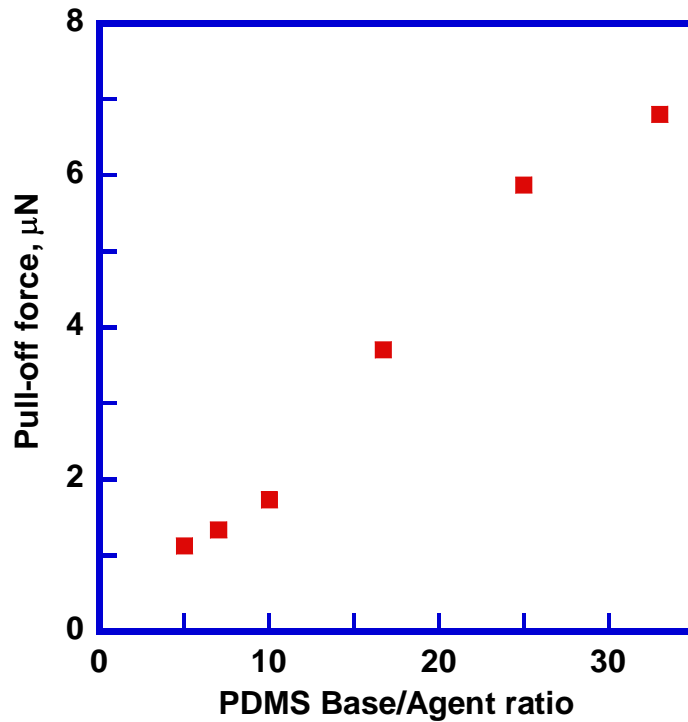
Figure 41. PDMS network pull-off force based on crosslinking.

Based to the JKR contact theory for spherical indentation:

$$P = \frac{4E^* a^3}{3R} - \sqrt{8\pi E^* a^3 \omega} \qquad (21).$$

where P is pull-off force, E^* is the reduced modulus, a is the contact radius, and R is the tip radius. ω is a general term that encompasses the work of adhesion [48]. So the adhesion force is related to the tip's geometric shape.

54

Also, the work of adhesion force is the integral of adhesion force on a certain depth interval. In Figure 38 and 40, the work of adhesion is also the area of pull-off force region. For example: the area of pull-off force region in Figure 38 is 35 μN*μm, so the work of adhesion in Figure 38 is 35E-12 J.
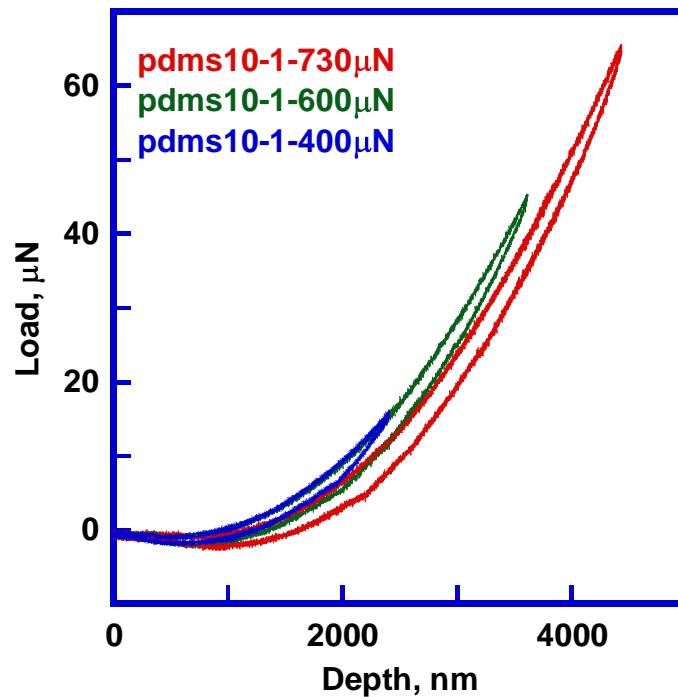
Figure 42.a. The pull-off forces based on PDMS network nanoindentation displacement.

Figure 42.a shows the relationship between PDMS network pull-off force and the samples' nanoindentation displacement. The pull-off force increases with the indentation depth. The same data is reorganized and shown in Figure 42.b. It is clear that the relationship between PDMS network pull-off forces and the samples' nanoindentation displacements is linear. This relationship can be described as:

$$Y=0.96533+0.00017201x, R=0.99975 \tag{22}$$

Y is the pull-off force, x is nanoindentation depth. Both are shown in Figure 42.c.

55
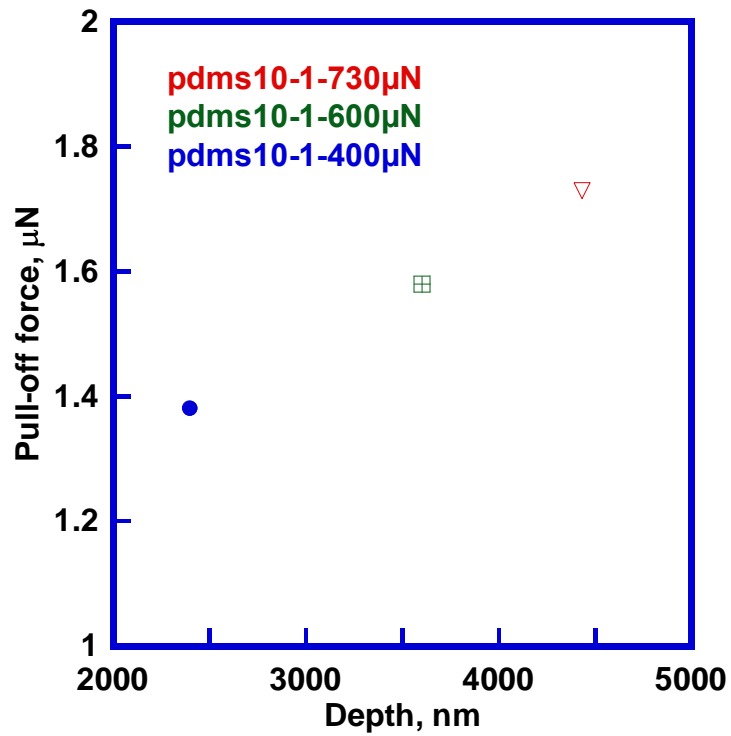
Figure 42.b. The pull-off forces data from Figure 42.a.
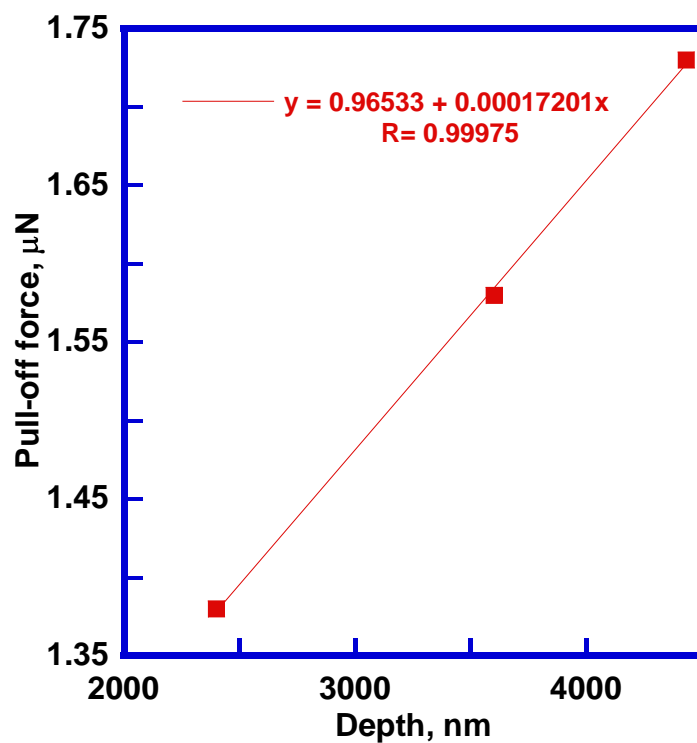
Figure 42.c. The linear curve fitting for pull-off forces from Figure 42.b.

56

Additional research was done for the relationship between the pull-off force and the nanoindentation unloading rate, shown in Figure 43.a and Figure 43.b. Regardless of whether the uploading time is 5 seconds or 10 seconds, the pull-off force doesn't change with the unloading rate.
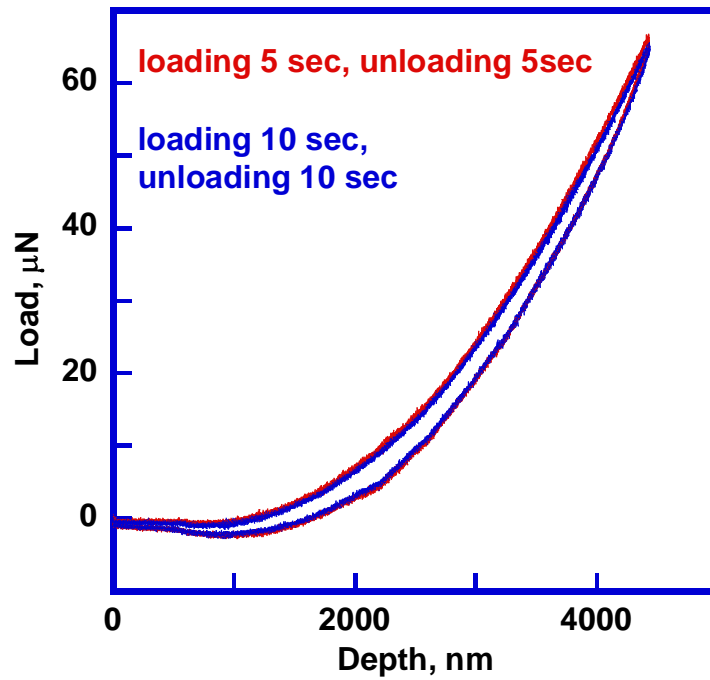
Figure 43.a. PDMS network 10:1 pull-off force based on the unloading rate.
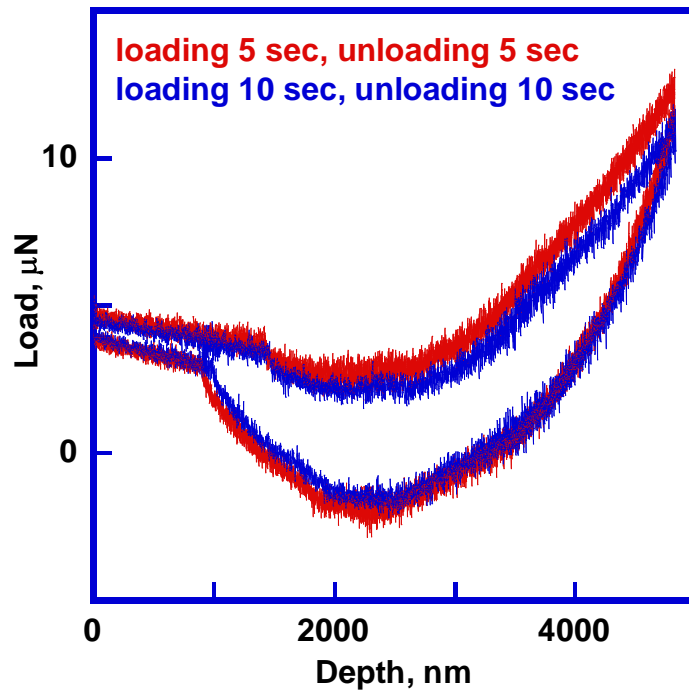
Figure 43.b. PDMS network 25:1 pull-off forces based on the unloading rate.

3.3.4 Adhesion Force - Conical Tip

The pull-off force is related to the geometry shape of the nanoindentation tip. [47] So additional nanoindentation experiments on adhesion force were done using the same procedure, but with a conical tip instead of a Berkovich tip. Conical tip is a spherical tip, which is different from the three surfaces Berkovich tip. Open loop control was used to do the test. Resulting data is shown in Figure 44.

www.manaraa.com
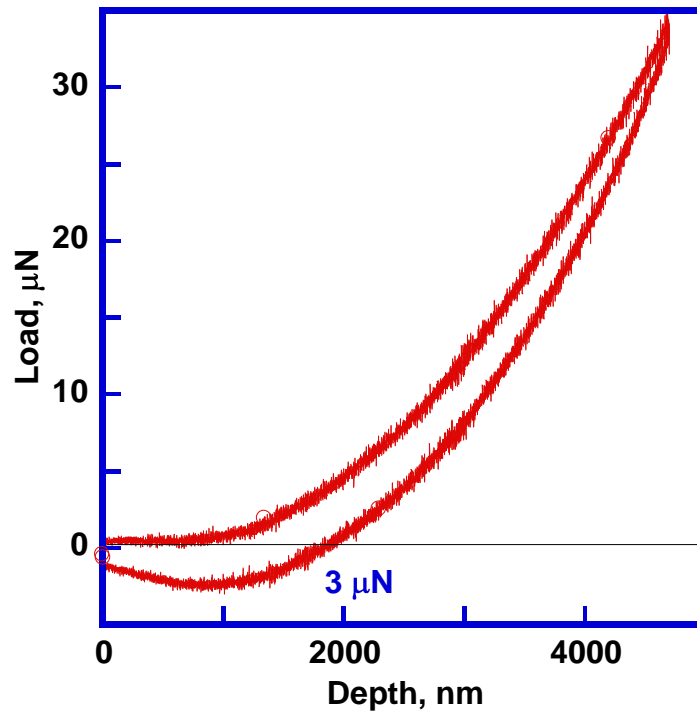
Figure 44. PDMS network nanoindentation adhesion force with the conical tip.

In Figure 44, PDMS network sample with base/agent ratio 5:1 was used for the experiment. There is no visible initial contact phenomenon, but one can see the pull-off force yielding when the tip leaves the sample surface. The pull-off force in Figure 44 is around 3 μN, while the pull-off force for PDMS network 5:1 in Figure 38 is around 35 μN. The difference between the pull-off force with the conical tip and the pull-off force with the Berkovich tip is due to the geometric shape of nanoindentation tips [47, 49].

3.3.5 Adhesion Force - Cube Corner Tip

Nanoindentation experiments on adhesion force were also done with a cube corner tip. The same open lop control was used to do the test. Collected data is shown in Figure 45.

In Figure 45, PDMS network sample with 5:1 base/agent ratio was used for experiments. There is no visible initial contact phenomenon, but one can see the pull-off force. The pull-off force is around 2 μN.
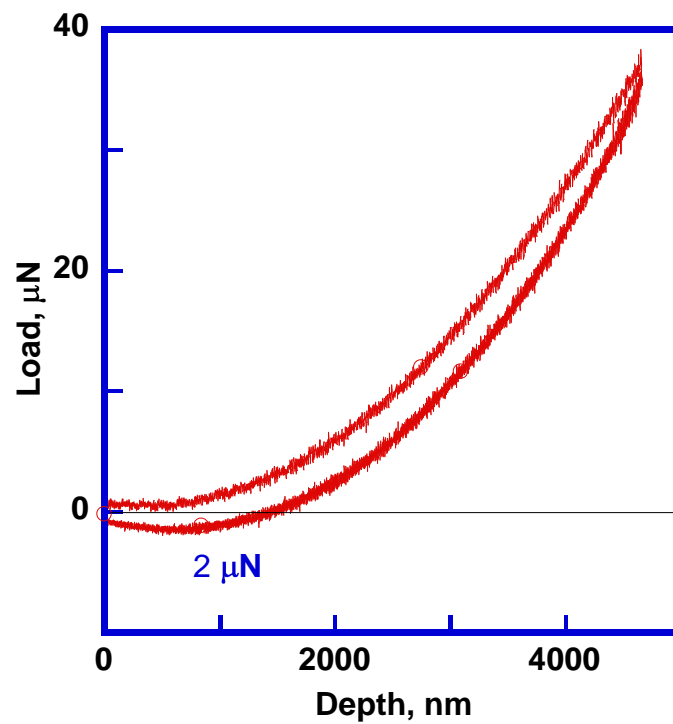
Figure 45.a. PDMS network 5:1 nanoindentation adhesion force test with the cube corner tip (Loading time: 2 sec. Unloading time: 5 sec).
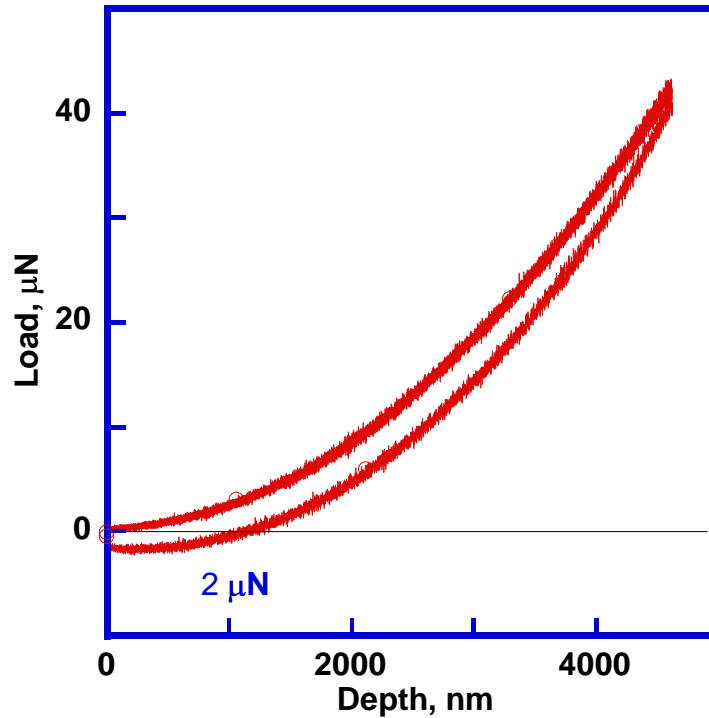
Figure 45.b. PDMS network 5:1 nanoindentation adhesion force test with the cube

corner tip (Loading time: 5 sec. Unloading time: 2 sec).

The differences between the experiment in Figure 45.a and the experiment in

Figure 45.b are the loading time and the unloading time. In the tests using a cube

corner tip, the loading and unloading ratios do not affect the adhesion force. In

equation (21), E^* is the same due to the same sample, so pull-off force P will depend

on the contact radius a and the tip radius R, which are all related to the tip's geometric

shape. Also, comparing with the pull-off force (35 μN) in PDMS network 5:1

Berkovich tip test and the pull-off force (3 μN) in PDMS network 5:1 conical tip test,

one can see the tip's geometric shape does influence the adhesion force [50].

61

3.4 Conclusions for Chapter 3

PDMS network nano-DMA tests provide stable data with different test models. The storage modulus is increasing when the test frequency. The loss modulus reaches a peak when the DMA test frequency is around the transducer's natural frequency. Also the data collected in nano-DMA test is comparable with the data collected in PDMS network compression test. Nanoindentation experiments with flat punch were also done to test the elastic modulus of PDMS network 5:1 and yield similar results.

Adhesion force experiments are done with different tips, which are Berkovich tip, cornical tip and cube corner tip. The adhesion forces are related to the PDMS network samples' base/agent ratios and the tips' geometrical shapes.

Chapter 4. Summary and Future Work

This research was done to explore the effect of substrate stiffness on the growth and behavior of cells attached to PDMS network substrates. In this thesis, the relationship between the elastic modulus of PDMS network and the base/agent ratio (the amount of crosslinking) is studied.

Most challenges of this research have been overcome. Reliable macroscopic compression test instrument was created. Preload method was applied for the nanoindentation flat punch test to develop full contact.

In chapter 2, a series of PDMS network samples with different base/agent ratios were tested with the macroscopic compression test. The elastic modulus of PDMS network 5:1 is 3.59 MPa, the elastic modulus of PDMS network 7:1 is 2.91 MPa, the elastic modulus of PDMS network 10:1 is 2.66 MPa, the elastic modulus of PDMS network 16.7:1 is 1.21 MPa, the elastic modulus of PDMS network 25:1 is 0.98 MPa, and the elastic modulus of PDMS network 33:1 is 0.78 MPa. The relationship between PDMS network elastic modulus and its base/agent ratio, n, is: $E=20/n$.

In chapter 3, PDMS network nano-DMA tests provide stable data with different test models. The storage modulus collected in nano-DMA tests is comparable with elastic modulus collected in PDMS network compression test in chapter 2. Elastic modulus of PDMS network 5:1 was also measured using flat punch quasi-static test. The adhesion force tests with different nanoindentation tips, respectively, Berkovich tip, conical tip, cube corner tip, show that PDMS's adhesion force is related to the

63

samples' base/agent ratios and the tips' geometrical shapes. Different properties and phenomena were studied with different systems of Hysitron Triboindentor. The elastic modulus in chapter 2 with compression test and in chapter 3 with flat punch nanoindentation test and nano-DMA test are comparable.

In future, DMA as a novel technique for soft polymer materials need to be better developed based on more research. Also, more base/agent ratios of the PDMS network samples need to be tested with both compression method and flat punch nanoindentation method to obtain more accurate PDMS network mechanical properties.

References

[1] L.H. Sperling, Introduction to Physical Polymer Science, Wiley-Interscience, New Jersey, 2006.

[2] C.R. Barrett. The Principles of Engineering Materials. Prentice Hall, 1973

[3] M.F. Ashby, Materials Selection in Mechanical Design, 3rd Edition. Elsevier 2005

[4] I. Wong, C.-M. Ho. Surface molecular property modifications for poly(dimethylsiloxane) (PDMS) based microfluidic devices. Microfluid Nanofluid (2009) 7:291–306

[5] D. Fuard, T. Tzvetkova-Chevolleau, S. Decossas, P. Tracqui, P. Schiavone. Optimization of poly-di-methyl-siloxane (PDMS) substrates for studying cellular adhesion and motility. Microelectronic Engineering 85 (2008) 1289–1293

[6] World wide web: http://en.wikipedia.org/wiki/Polydimethylsiloxane. 2011.

[7] Information about Dow Corning® Brand Silicone Encapsulants. Product Information. Dow Corning and Sylgard are registered trademarks of Dow Corning Corporation. ©2000-2008 Dow Corning Corporation. All rights reserved. Form No. 10-898I-01

[8]http://www.csflab.com/wiki/index.php?title=Quantification_of_the_Modulus_of_Elasticity_and_Dynamic_Properties_of_Sylgard_for_Various_Mixing_Ratios,_2003-2006. 2009.

[9] Hysitron Triboindenter Manual. 2000. Hysitron company.

[10] J. Lemaitre and J.L. Chaboche. Mechanics of Solid Materials. Cambridge University Press. 1990.

[11] World wide web: http://www.ptli.com/testlopedia/tests/Compression-d695.asp. Entire contents © 1996-2011 Intertek Plastics Technology Laboratories.

[12] M. VanLandingham, Review of instrumented indentation, J Res Natl Inst Stand Technol 108 (2003), pp. 249–265.

[13] W.C. Oliver and G.M. Pharr, An improved technique for determining hardness and elastic modulus using load and displacement sensing indentation experiments, J Mater Res 7 (1992), pp. 1564–1583.

[14] J.K. Deuschle, G. Buerki, H. Matthias Deuschle, S. Enders, J. Michler, E. Arzt. In situ indentation testing of elastomers, Acta Materialia 56 (2008) 4390-4401.

[15] R.C. Hibbeler, Mechanics of Materials, Prentice Hall. 1997.

[16] D.C. Duffy, J. Cooper McDonald, Olivier J.A. Schueller and G.M. Whitesides. Rapid Prototyping of Microfluidic Systems in Poly(dimethylsiloxane), Anal. Chem. 70, 1998. pp. 4974-4984.

[17] ASM Handbook, Vol. 8, Mechanical Testing and Evaluation, ASM International, Materials Park, OH 44073-0002

[18] Oliver WC, Pharr GM. An improved technique for determining hardness and elastic modulus using load and displacement sensing indentation experiments. J Mater Res (1992);7:1564.

[19] J.G. Jacot, S. Dianis, J. Schnall and J. Y. Wong. A simple microindentation technique for mapping the microscale compliance of soft hydrated materials and tissues J. Biomed. Mater. Res. A 79 (2006) 485–94

[20] G.M. Odegard, H.M. Herring, T.S. Gates. Characterization of Viscoelastic Properties of Polymeric Materials through Nanoindentation. 2005 Society for Experimental Mechanics. Vol. 45, No. 2, April 2005.

[21] I. Levental, K.R. Levental, E.A. Klein, R.T. Miller, R.G. Wells and P.A. Janmey. A simple indentation device for measuring micrometer-scale tissue stiffness. J. Phys.: Condens. Matter 22 (2010) 194120 (9pp)

[22] Y.T. Cheng, C.M. Cheng. Scaling, dimensional analysis, and indentation measurements. Mater Sci Eng R 2004;44:91.

[23] F. Carrillo, S. Gupta, M. Balooch, S.J. Marshall, G.W. Marshall, L. Pruitt, C.M. Puttlitz. Nanoindentation of polydimethylsiloxane elastomers: Effect of crosslinking, work of adhesion, and fluid environment on elastic modulus. J. Mater. Res., Vol. 20, No. 10, Oct 2005.

[24] S.C. Tjong. Structural and mechanical properties of polymer nanocomposites. Materials Science and Engineering R 53 (2006) 73–197.

[25] H. Schmid and B. Michel. Siloxane Polymers for High-Resolution, High-Accuracy Soft Lithography. Microelectronic Engineering 69 (2003) 519–527

[26] W.C. Hayes, L.M. Keer, G. Herrmann and L.F. Mockros, A mathematical analysis for indentation tests of articular cartilage, J Biomech 5 (1972), pp. 541–551.

[27] W. Nix, Elastic and plastic properties of thin films on substrates: Nanoindentation techniques, Material Science and Engineering A234-236 (1997) 37-44.

[28] S.M. Han, R. Saha and W.D. Nix. Determining hardness of thin films in elastically mismatched film-on-substrate systems using nanoindentation. Acta Mater 54 (2006) 1571-1581.

[29] J.M. Meza, Penetration depth and tip radius dependence on the correction factor in nanoindentation measurements, J. Mater. Res., Vol.23, No.3. Mar 2008.

[30] K. Du, Novel Nanoindentation-Based Techniques for MEMS and Microfluidics Application, M.S. Thesis, University of South Florida, Florida, 2008.

[31] G. Gorrasi, L. Guadagno, C. D'Aniello, C. Naddeo, G. Romano, V Vittoria. Recognition of the Syndiotactic Polypropylene Polymorphs via Dynamic-mechanical Analysis, Macromol. Symp., 2003, 203, 285-294.

[32] T. Murayama, Dynamic Mechanical Analysis of Polymeric Materials, Elsevier: New York, 1978.

[33] G. M. Odegard, T. Bandorawalla, H.M. Herring and T.S. Gates. Characterization of Viscoelastic Properties of Polymeric Materials through Nanoindentation. Experimental Mechanics, Vol. 45, No. 2, 130-136 (2005).

[34] L. Cheng X. Xia, W. Yu, L. E. Scriven and W. W. Gerberich. Flat Punch Indentation of Viscoelastic Material, J of Polymer Sci Part B: Polymer Phy., 38, 10-22, 2000.

[35] S. P. Singh, R. P. Singh and J. F. Smith. Displacement Modulation Based Dynamic Nanoindentation for Viscoelastic Material Characterization. Mater. Res. Soc. Symp. Proc. Vol. 841 2005.

[36] S.A. Syed Asif, K.J. Wahl and R.J. Colton, Nanoindentation and Contact Stiffness Measurements Using Force Modulation with a Capacitive Load-displacement Transducer. Review of Scientific Instruments, 70, 2408-2413 (1999).

[37] J.L. Loubet, W.C. Oliver, and B.N. Lucas, "Measurement of the Loss Tangent of Low-density Polyethylene with a Nanoindentation Technique," Journal of Materials Research, 15, 1195-1198 (2000).

[38] H. Lu, B. Wang and G. Huang, "Measurement of Complex Creep Compliance Using Nanoindentation," 2003 SEM Annual Conference and Exposition on Experimental and Applied Mechanics, Charlotte, NC (2003).

[39] B. Erman, J.E. Mark, Structures and Properties of Rubberlike Networks; Oxford University Press: Oxford, 1997.

[40] J.A. Hammerschmidt and W.L. Gladfelter. Probing Polymer Viscoelastic Relaxations with Temperature-Controlled Friction Force Microscopy. Macromolecules, 1999, *32* (10), pp 3360–3367

[41] Y. Cao, D. Ma and D. Raabe. The use of flat punch indentation to determine the viscoelastic properties in the time and frequency domains of a soft layer bonded to a rigid substrate. Acta Biomaterialia 5 (2009) 240–248.

[42] K. Du, X. Pang, C. Chen, and A.A. Volinsky. Mechanical Properties of Evaporated Gold Films. Hard Substrate Effect Correction. Mater. Res. Soc. Symp. Proc. Vol. 1086, 2008.

[43] X. Pang, K. Gao, F. Luo, H. Yang, L. Qiao, Y. Wang, A.A. Volinsky. Annealing effects on microstructure and mechanical properties of chromium oxide coatings. Thin Solid Films 516 (2008) 4685–4689.

[44] A.A. Volinsky, W.W. Gerberich. Nanoindentaion techniques for assessing mechanical reliability at the nanoscale. Microelectronic Engineering 69 (2003) 519–527

[45] J. Deuschle, S. Enders, and E. Arzt, Surface detection in nanoindentation of soft polymers J. Mater. Res. 22(2007) 3107–19

[46] D.M. Ebenstein and L.A. Pruitt, Nanoindentation of soft hydrated materials for application to vascular tissues, J Biomed Mater Res A 69 (2004), pp. 222–232.

[47] Y.T. Cheng and C.M. Cheng, General relationship between contact stiffness, contact depth, and mechanical properties for indentation in linear viscoelastic solids using axisymmetric indenters of arbitrary profiles, Appl Phys Lett 87 (2005), p. 111914.

[48] Y.Y. Lin, C.Y. Hui and J.M. Baney. Viscoelastic contract , work of adhesion and the JKR technique. J. Phys. D: Appl. Phys. 32 (1999) 2250–2260.

[49] B.J. Briscoe, L. Fiori and E. Pelillo, Nano-indentation of polymeric surfaces, J Phys D – Appl Phys 31 (1998), p. 2395.

[50] K.L. Johnson. Surface energy and the contact of elastic solids, Proc. R. Soc. London A 324 (1971) 301-313